A General Strategy for Highly Efficient Nanoparticle Dispersing Agents Based on Hybrid Dendritic Linear Block Copolymers

ROBERT VESTBERG,[1,2] ASHLEY M. PIEKARSKI,[1,2] ERIC D. PRESSLY,[1] KIM Y. VAN BERKEL,[1] MICHAEL MALKOCH,[1] JEFFREY GERBAC,[3] NOBUHIKO UENO,[4] CRAIG J. HAWKER[1,2]

[1]Materials Research Laboratory, University of California, Santa Barbara, California 93106

[2]Mitsubishi Chemical Center for Advanced Materials, University of California, Santa Barbara, California 93106

[3]Mitsubshi Chemical Research and Innovation Center, 601 Pine Avenue, Suite C, Goleta, California 93117

[4]Mitsubshi Chemical Research Center, 1000 Kamoshida-Cho, Aoba-Ku, Yokohama 227-8502, Japan

Received 12 September 2008; accepted 4 November 2008
DOI: 10.1002/pola.23186
Published online in Wiley InterScience (www.interscience.wiley.com).

ABSTRACT: A modular approach to the synthesis of a library of hybrid dendritic-linear copolymers was developed based on RAFT polymerization from monodisperse dendritic macroRAFT agents. By accurately controlling the molecular weight of the linear block, generation number of the dendrimer and the nature of the dendritic chains ends, the performance of these hybrid block copolymers as dispersing agents was optimized for a range of nanoparticles. For titanium dioxide nanoparticles, dispersion in a poly(methyl methacrylate) matrix was maximized with a second generation dendrimer containing four carboxylic acid end groups, and the quality of dispersion was observed to be superior to commercial dispersing agents for TiO_2. This approach also allowed novel hybrid dendritic-linear dispersing agents to be prepared for the dispersion of Au and CdSe nanoparticles based on disulphide and phosphine oxide end groups, respectively. © 2009 Wiley Periodicals, Inc. J Polym Sci Part A: Polym Chem 47: 1237–1258, 2009
Keywords: block copolymers; dendrimers; dispersions; surfaces

INTRODUCTION

The efficient dispersion of nanoparticles in matrix materials is becoming an important aspect of many emerging technologies, and the development of a general strategy for enhancing and maximizing the efficiency of dispersion will offer significant advantages in a variety of academic and industrial applications. For example, the thermomechanical response of polymers, which can limit the practical use of polymeric materials, are favorably altered by the addition of trace amounts of nanoparticles.[1] Similarly, the addition of high refractive index nanoparticles to polymeric materials can lead to a dramatic increase in the refractive index of the overall nanocomposite.[2] In both cases, the level and utility of property enhancement is directly related to the degree of dispersion for the nanoparticle. Nonuniform

Correspondence to: C. J. Hawker (E-mail: hawker@mrl.ucsb.edu)

Journal of Polymer Science: Part A: Polymer Chemistry, Vol. 47, 1237–1258 (2009)

dispersion leading to nanoparticle aggregation is detrimental as it results in undesirable properties such as the development of opacity in optical nanocomposites. Traditional approaches to nanoparticle dispersion involve the use of either small molecule ligands/surfactants[3] or functionalized polymers such as block copolymers.[4] However, a number of challenges exist with these dispersing agents. For small molecule derivatives, low dispersion efficiency is often obtained due to the lack of entanglements and favorable interactions with the polymeric matrix. In contrast, polymeric dispersing agents can have favorable interactions and entanglements with the polymeric matrix, but the loading levels of these materials is often extremely high and is further exacerbated by the high surface area of nanoparticle systems. The weight percentage of the dispersing agent then becomes significant and leads to decreased performance.

A significant opportunity therefore exists to develop a general approach to the design of dispersing agents that combine the specificity and high binding strength of small molecules with the favorable interactions of polymeric dispersants. To address these issues, new dispersing agents were designed based on macromolecular architectures which optimally present, both surface active groups for attaching to the surface of the nanoparticle, and matrix interacting groups which promote dispersion in polymeric matrices. Hybrid dendritic linear block copolymers[5–8] satisfy these criteria with the dendritic unit being used as the "head" group to interact with the nanoparticle surface while the linear block is able to entangle and interact with the polymeric matrix. Dendritic macromolecules have found extensive use as stabilizing nanoreactors for nanoparticle formation[9(a,b)] or functionalization of nanoparticle surfaces.[9(c)] However, no studies have been reported describing the use of hybrid dendritic linear block copolymers to stabilize the surface of nanoparticles even though the surface activity of dendrimers is well noted and the presence of the linear block offers a number of interesting opportunities.[10] In particular, the numerous reactive groups at the chain ends of the dendrimer have been shown to lead to an optimal conformation for interacting with surfaces.[11–14] The absence of chain folding and chain dynamics when compared to functionalized linear chains is also expected to lead to a much stronger interaction with, and greater coverage of the nanoparticle at significantly lower loading of the copolymer. Previously,

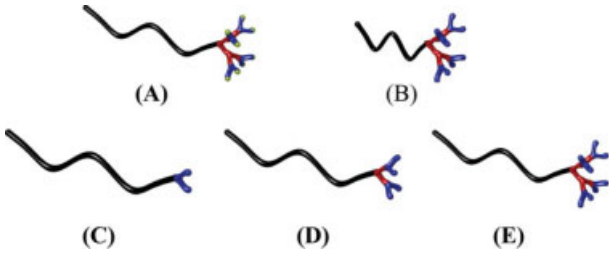

Figure 1. Graphical representation of modular changes in the structure of hybrid dendritic-linear diblock copolymers through varying the nature of the end groups (A to E), length of linear block (B to E), or via the changing the generation number of the dendritic block, [G-1], [G-2], and [G-3] (C to D to E, respectively).

Frechet et al.[15] has shown that poly(ethylene glycol)-based hybrid dendritic macromolecules can cover the surface of cellulose fibers at very low concentrations due to a combination of self-assembly and physisorption. In this article, we present the design and synthesis of modular dendritic-linear hybrid copolymers in which the nature of both the dendritic chain end groups, as well as the repeat units of the linear polymer chain, can be easily varied. The ability of these materials to efficiently disperse a range of nanoparticles in polymeric matrices is also demonstrated. Of particular note is the modular nature of dendrimers which allows the nature and length of the linear polymer and/or functional groups at the chain end of the dendrimers to be simply varied and permits the tailoring of this strategy to essentially any nanoparticle and matrix combination (Fig. 1).

RESULTS AND DISCUSSION

In designing hybrid dendritic-linear block copolymers, dendrimers based on 2,2-bis(methylol)propionic acid (bisMPA)[16] were chosen because of their commercial availability[17] and widespread use, while the linear chain was based on vinyl polymers prepared by reversible addition fragmentation chain transfer polymerization (RAFT).[18,19] The synthesis of the dendritic macroRAFT agent starts from the *N*,*N*′-dicyclohexylcarbodiimide (DCC)-mediated esterification of the acetonide protected trimethylol propane, **1**, with α-bromophenylacetic acid, **2**. Coupling of **3** and the anion of dithiobenzoic acid, which is prepared from the reaction of phenylmagnesium bromide with carbon disulfide, then gives the desired dithioester,

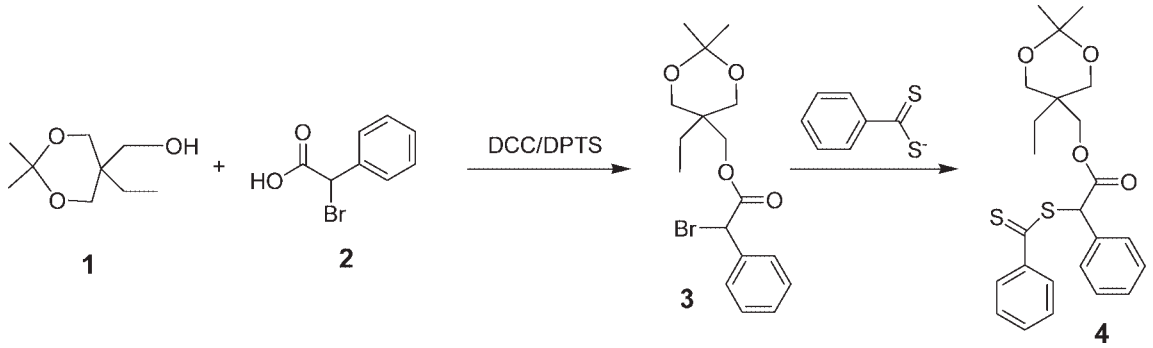

Scheme 1. Synthesis of first generation RAFT agent, **4**, for growth of dendritic macroRAFT agents.

4, in an overall yield of greater than 90% (Scheme 1).[20]

The stability of the dithioester macroRAFT agent to functional group manipulation was then demonstrated by divergently growing dendritic units from **4** through a traditional series of deprotection and coupling reactions (Scheme 2). The deprotection reactions were performed utilizing acidic Dowex resins in methanol[21] and the addition reactions accomplished by esterification of the hydroxyl chain ends with the anhydride of the acetonide-protected bisMPA.[22] Both steps proceed readily with purified yields of over 90% for 10–20 g batches which allowed dendrons of the first, **5**, to the fourth generation, **6**, to be prepared with a single dithioester RAFT agent at the focal point.

In the next step, polymers are grown from the single dithioester group at the focal point of the dendrimer by RAFT polymerization. Because of the presence of both a phenyl substituent and ester group attached to the α-carbon of the dithioester, these dendritic macroinitiators can be used for polymerization of a variety of monomers including methacrylates with AIBN as the initiator at 70 °C in the bulk (Scheme 3) or styrene at 110 °C in the bulk with no added AIBN (Scheme 4). In each case, the efficiency of polymerization from the macroRAFT agent was found to be 75–95% depending on the generation number, and the actual percentage could be uniquely identified and quantified due to the narrow GPC peak for the starting macroRAFT agent. The high solubility of the dendritic macroRAFT agent was also beneficial during purification as it allowed the block copolymer to be purified by simple precipitation and/or column chromatography and the lack of residual macroRAFT agent confirmed by GPC (Fig. 2). Of particular note is the observation that all polymerizations occurred under controlled conditions that allows for the degree of polymerization of the linear block to be accurately controlled. This affords a range of hybrid dendritic-linear block copolymers in which the length of the linear chain and the generation number of the dendritic block could be dictated (Table 1).

The modular nature of this synthetic approach is further exemplified by manipulation of the chain end groups. To this end, the acetonide-protected end-groups of the starting hybrid dendritic-linear systems, **8**, were quantitatively removed with acidic Dowex resin to give hydroxyl-functional dispersing agents, **9**. The hydroxyl groups could then be reacted with succinic anhydride to yield carboxylic acid-substituted dispersing agents, **10** (Scheme 5).

To broaden the range of nanoparticles that could be dispersed using this modular system, modification of the dendritic chain end was accomplished by esterification of the hydroxyl chain ends using anhydride chemistry. To demonstrate this critical feature, Au and CdSe nanoparticles were chosen as test vehicles due to their specific surface chemistry. For Au nanoparticles, a dispersing agent with thioctic ester chain ends was prepared by reacting the hydroxyl chain ends of **9** with the anhydride derived from (±)-thioctic acid, **11**, to give the tetra(disulphide) derivative, **12** (Scheme 6).

In a similar vein, hybrid dispersing agents were designed for CdSe nanoparticles and in this case, phosphine oxide chain ends were required for interaction with the surface of the CdSe. Using an anhydride functionalization approach requires 5-(dioctylphosphoryl)pentanoic anhydride, **13**, which was synthesized by initial alkylation of di-*n*-butyl phosphate, **14**, with octylmagnesium iodide followed by reaction with 4-pentenoic acid using AIBN to give 5-(dioctylphosphoryl)

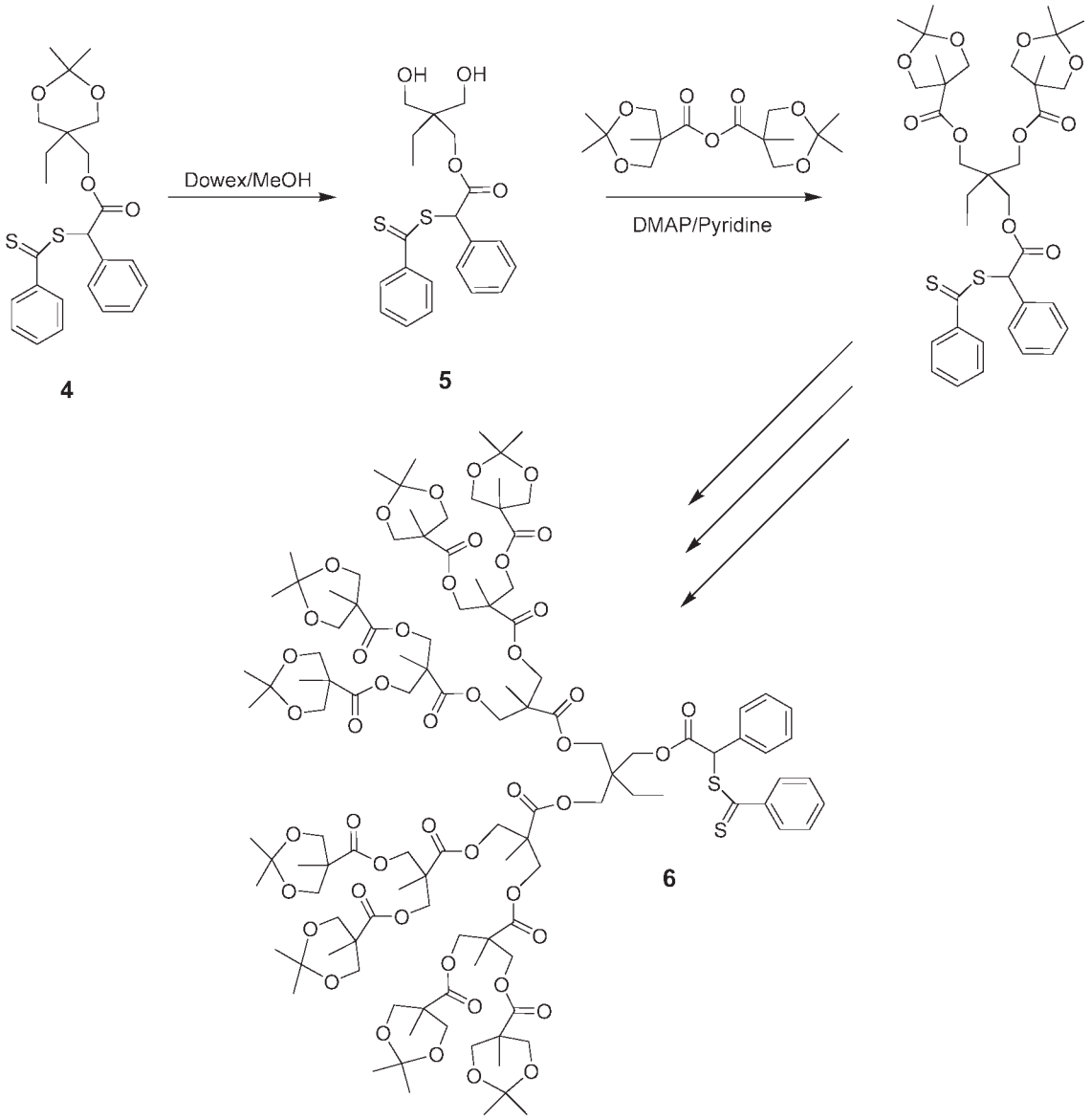

Scheme 2. Synthesis of dendritic macroRAFT agents, that is, [G-4] **6**, with a single dithioester RAFT agent at the focal point.

pentanoic acid, **15,** and final conversion to the desired anhydride, **13**, using DCC (Scheme 7). The anhydride was then used to functionalize the chain ends of **9a** to give the phosphine oxide functionalized dendritic-linear copolymer, **16** (Scheme 8).

In all the above examples, the hybrid dendritic-linear block copolymers were fully characterized by NMR and MALDI spectroscopy coupled with GPC. The well-defined structure of these derivatives allows accurate identification and quantification of the number and nature of the chain end groups which was found to be in full agreement with the synthetic strategy. For example, Figure 3 shows the ^{1}H and ^{31}P NMR data for the phosphine oxide functionalized dispersing agent ((Phosphine oxide)$_4$-[G-2]-PMMA, **16**), and a unique resonance for the methylene group alpha to the carbonyl is observed at 2.25 ppm in the ^{1}H NMR spectrum while a single resonance is observed in the ^{31}P NMR spectrum corresponding with four equivalent phosphine oxide groups.

A critical feature of the chain end modification chemistry and associated modularity of this strategy is to ensure that all the end groups of the dendritic dispersing agent are functionalized with

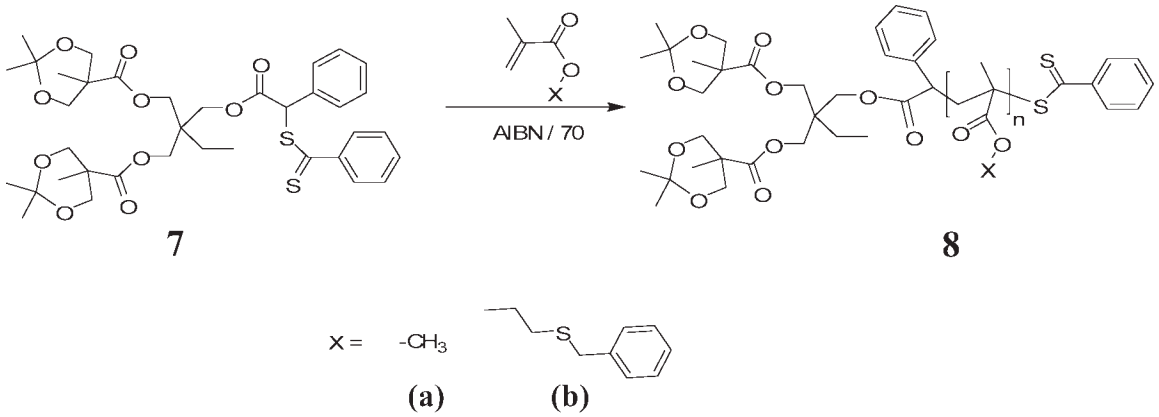

Scheme 3. RAFT polymerization of methacrylate monomers with a second generation dendritic macroRAFT agent, **7**.

high efficiency and few, if any, side reactions. While esterification using anhydride chemistry was shown to lead to high levels of functionalization, the synthesis of phosphonic acid end groups which are highly desirable for a variety of nanoparticle surfaces could not be accomplished using this strategy. To further expand the array of possible chain ends, an orthogonal approach was developed based on the copper (I) catalyzed 1,3-dipolar cycloaddition between azides and terminal acetylenes (Click reaction) which is more tolerant of reactive functional groups.[23] To illustrate the versatility of this approach, the introduction of phosphonic acid end groups via Click chemistry[24] was investigated by first introducing an azide endgroup through esterification of the hydroxyl chain ends with the anhydride derived from 4-azidobutanoic acid, **17**. The corresponding acetylene derivative was then prepared by reaction of propargyl alcohol with phosphoric acid/iodide in triethylamine followed by coupling with the azido-terminated derivative, **18**, to give directly the desired phosphonic acid functionalized hybrid dendritic-linear diblock copolymers, **19** (Scheme 9).[25]

Dispersion Studies

The synthesis of a library of hybrid dendritic-linear dispersing agents with accurate control over a range of structural features then allowed the dispersion activities of these novel systems to be studied in detail. As an initial test platform, the dispersion of TiO_2 nanoparticles in a high molecular weight poly(methyl methacrylate) matrix was examined in detail. For all the dispersing experiments, a planetary ball mill and Zirconia milling jars with 3 mm zirconia grinding balls were used. Initially 50 wt % of the total polymer and the dispersing agent is added to the milling jar followed by 50 wt % of the solvent, the TiO_2 nanoparticles, and the milling beads. This mixture is milled for 1 h at 650 rpm, the remaining polymer and solvent is then added, and milling continued for 1 h at 650 rpm (Fig. 4).

The dispersing experiments were carried out in chloroform (20 wt % solids) with commercially available TiO_2 nanoparticles with (TTO-51(A)) and without (TTO-51N) a surface coating of alumina in a matrix of PMMA (150,000 Da). The nanoparticle dispersions were analyzed with

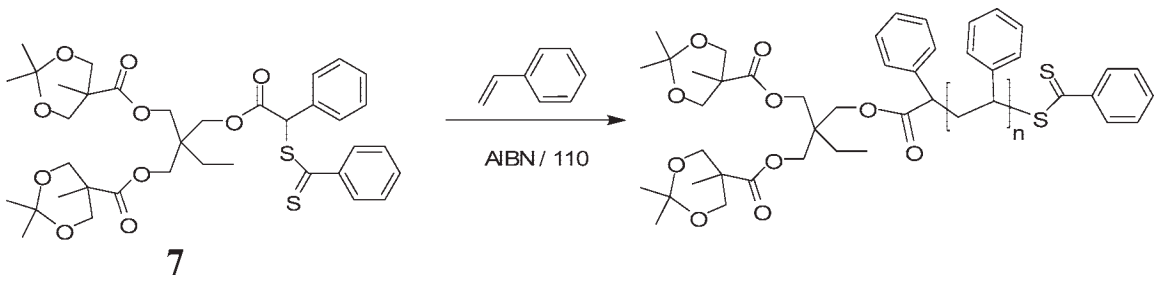

Scheme 4. RAFT polymerization of styrene with a second generation dendritic macroRAFT agent, **7**.

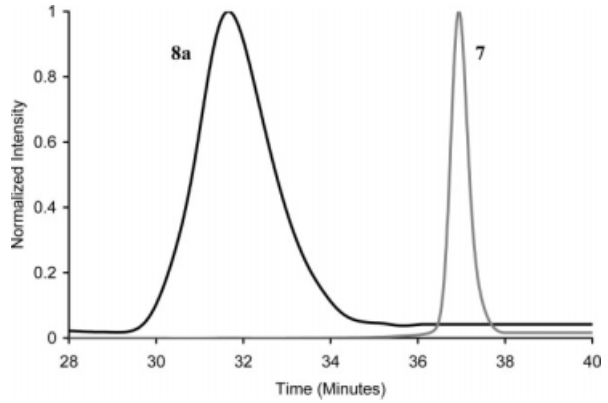

Figure 2. Size exclusion chromatographs for the hybrid dendritic-linear block copolymer, **8a** (M_n = 6200, PDI = 1.19) obtained from the RAFT polymerization of methyl methacrylate with the second generation dendrimer, **7** (MW = 716).

dynamic light scattering (DLS), transmission electron microscopy (TEM), and rheometrical studies. For evaluation purposes, the performance of the hybrid dendritic-linear dispersing agents were compared with the commercially available Disperbyk-111, Disperbyk-170, Disperbyk-180, dispersing agents that have found wide use for the preparation of composites based on inorganic nanoparticles such as TiO_2.

Initial TEM studies showed that in the absence of any dispersing agents, both types of TiO_2 nanoparticles led to large clusters of nanoparticles being observed which is expected due to the large surface area of the nanoparticles and poor compatibility with poly(methyl methacrylate) (Fig. 5). Similar results were observed for two of the commercial dispersing agents (Disperbyk-170 and Disperbyk-180, Fig. 6) while the Disperbyk-111 showed better results with high-quality dispersions being observed for a variety of different concentrations (Fig. 7).

For the hydroxyl, carboxy, and phosphonic acid-terminated hybrid dendritic-linear dispersing agents, a series of dendrimers of generations 1–3, with a uniform PMMA block of DP $\sim$ 50, were initially examined and compared to determine the optimal generation number for the dendritic head group. For each series the level of dispersion increased on going from generation 1 to generation 2 and then decreased on going to generation 3 and this progression can be visually seen in Figure 8. This optimum size for the dendritic head group of generation 2 is similar to the pioneering studies from Fréchet on the adsorption of dendritic-linear copolymers to the surface of PET and cellulose.[9] Comparison between the different series showed a significant influence because of the nature of the end group, the hydroxyl-terminated derivatives showed only marginal dispersing activity with the majority of nanoparticles being present as aggregates. Similarly, the phosphonic acid-terminated hybrid structures gave improved performance but a mixture of aggregates and individual nanoparticles could still be observed (Fig. 9). Only for the dendritic-linear block copolymers with carboxy chain ends is a high degree of dispersion observed with individual nanoparticles and small aggregates predominating. Of particular note is the comparison with the best performing commercial dispersing agent, Disperbyk-111, which under the same dispersing conditions showed quantitatively poorer performance when compared to **10a** (Fig. 10).

Table 1. Polymerization of Different Generation CTAs

Generation Number	Monomer	Reaction Time (h)	Conversion	M_n	PDI
1	MMA	5:30	75	25,400	1.13
2	MMA	4:30	67	27,700	1.13
3	MMA	5:10	84	27,300	1.15
4	MMA	4:00	65	24,600	1.13
1	MMA	2:55	53	5,010	1.21
2	MMA	1:40	65	5,190	1.24
3	MMA	1:25	84	5,880	1.23
1	Bz-TEMA	0:50	87	14,100	1.1
2	Bz-TEMA	1:10	86	14,400	1.12
3	Bz-TEMA	1:40	81	16,000	1.12
2	Bz-TEMA	1:00	84	26,200	1.29
2	Styrene	28:00	72	7,300	1.05
2	Styrene	28:00	74	39,200	1.14

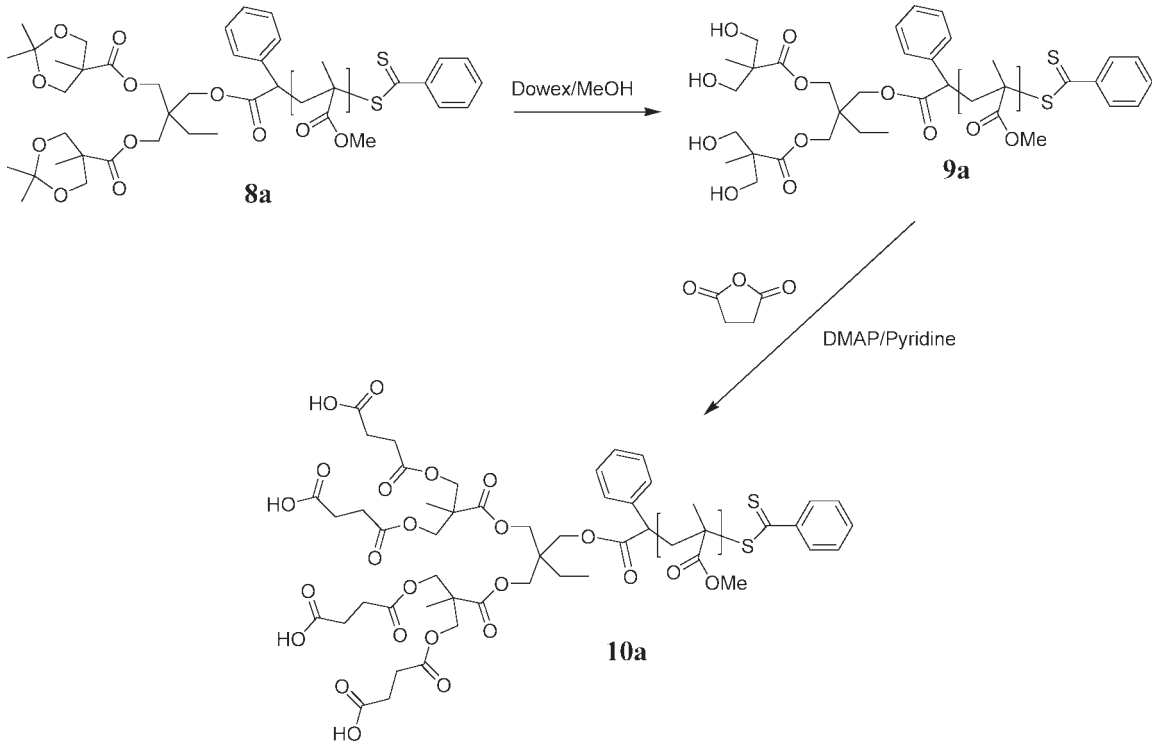

Scheme 5. Synthesis of carboxy-terminated hybrid dendritic-linear block copolymers, **10a**, by deprotection of the corresponding acetonide derivative, **8a**, followed by functionalization of the alcohol, **9a**, with maleic anhydride.

A further gauge of the qualitative performance of the hybrid dendritic-linear dispersants was obtained from a systematic study of the viscosity versus concentration of solids (10–30% of solids in $CHCl_3$) for the different dispersing agents. As can be seen in Figure 11, the viscosity of nanoparticle suspensions was reduced marginally by the use of the commercial dispersing agent, Disperbyk-170. In contrast, both the Disperbyk-111 and the hybrid structure based on a linear PMMA chain and a second generation dendrimer with carboxylic acid end group gave significantly lower viscosities which again demonstrates good dispersion and the lack of large nanoparticle aggregates.

To obtain quantitative data for the performance of the hybrid dendritic-linear macromolecules as dispersing agents, dynamic light scattering (DLS) was used as a complement to the TEM measurements. The samples were therefore diluted to 0.5% of the original concentration for the DLS measurements and the intensity correlation functions were collected at five different angles (30°,

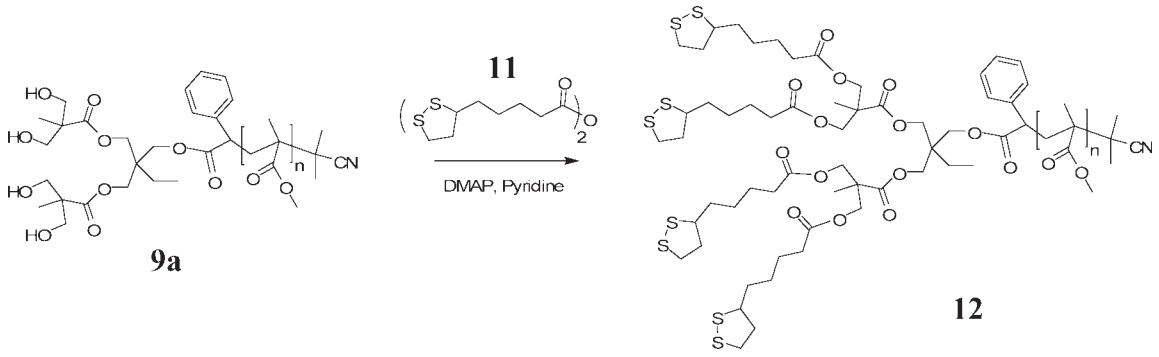

Scheme 6. Synthesis of disulphide-terminated hybrid block copolymers, **12**, for dispersion of Au nanoparticles.

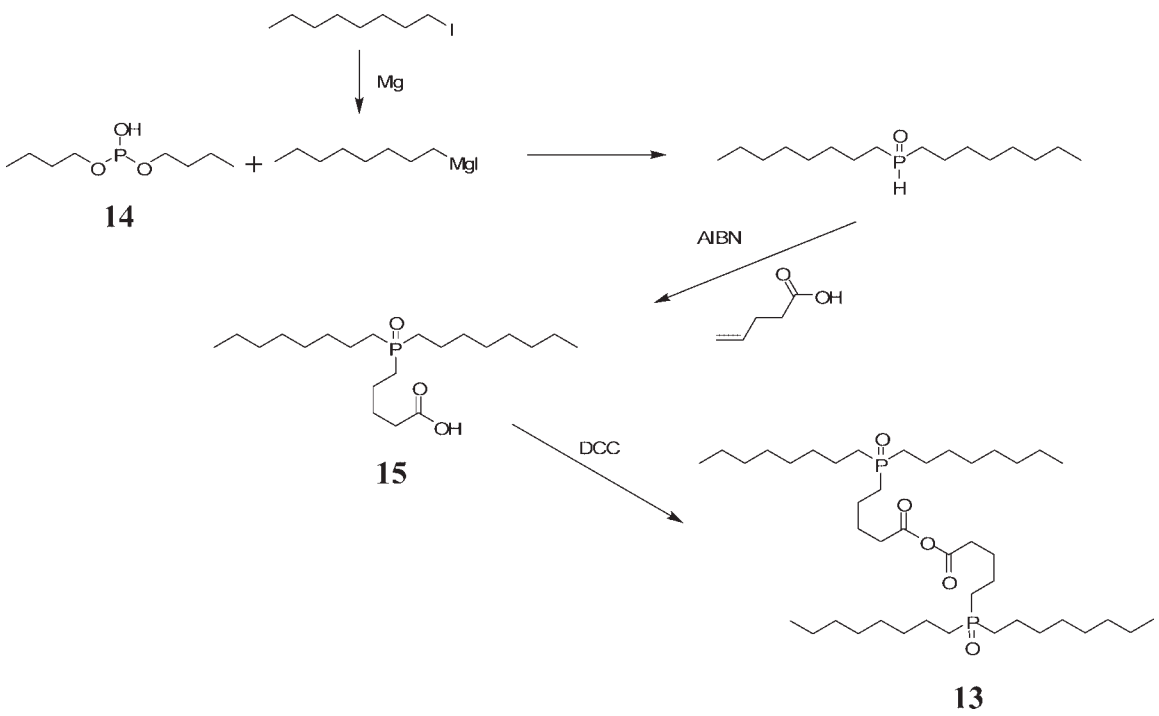

Scheme 7. Synthesis of 5-(dioctylphosphoryl)pentanoic anhydride, **13**.

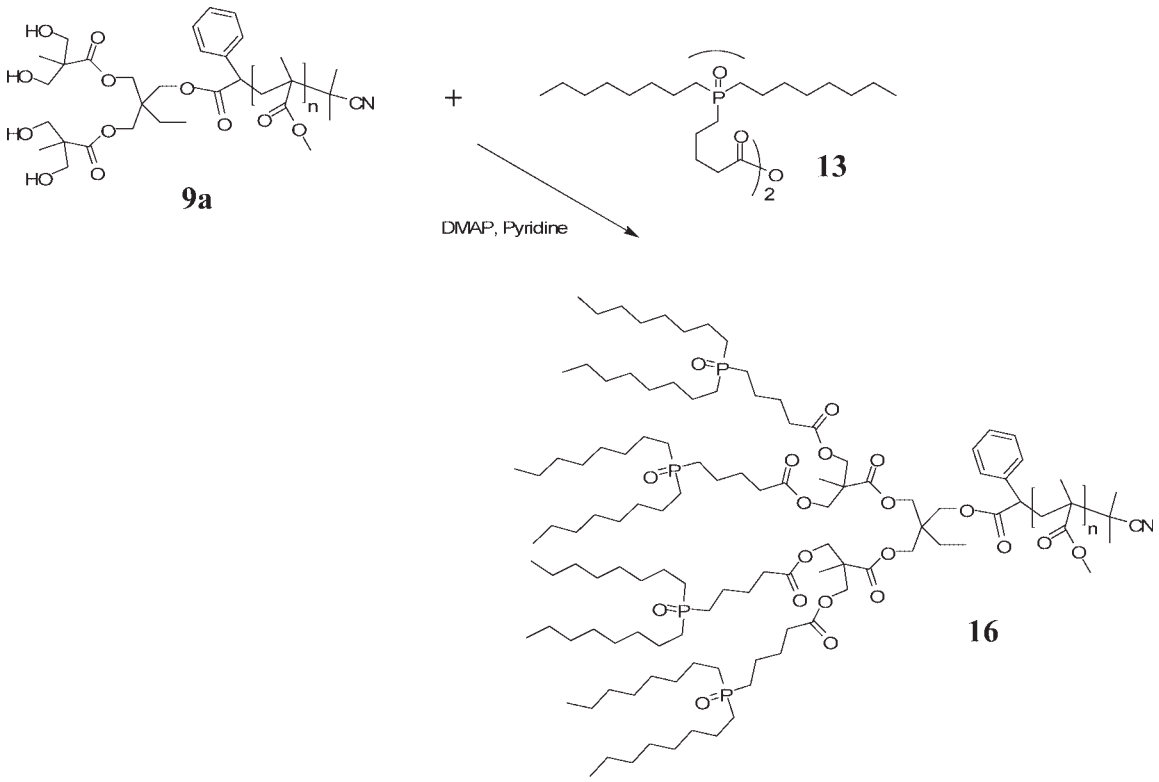

Scheme 8. Synthesis of tetrafunctional phosphine oxide PMMA derivative, **16**.

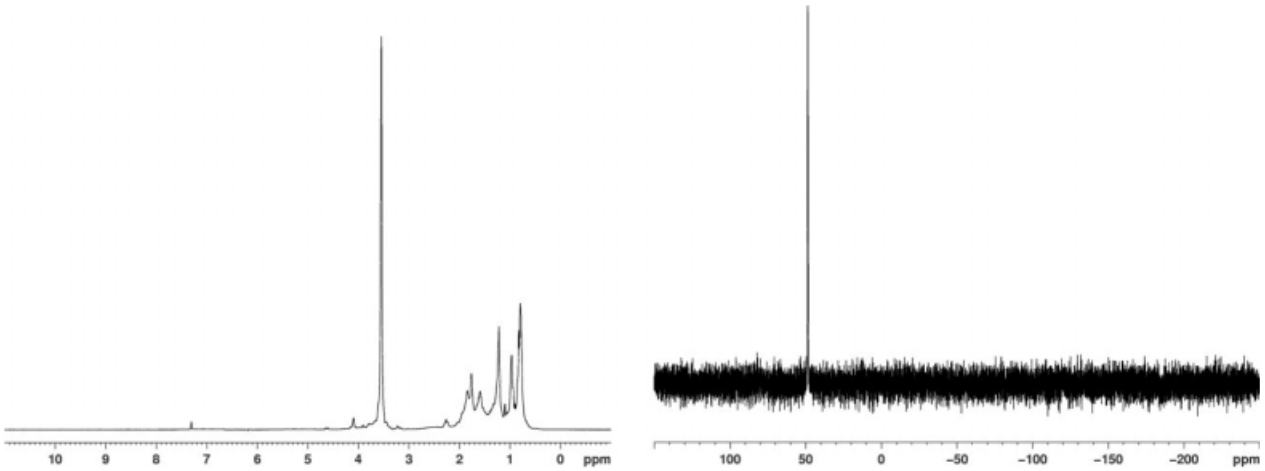

Figure 3. ^{1}H (left) and ^{31}P (right) NMR spectra of (phosphine oxide)$_4$-[G-2]-PMMA, **16**.

60°, 90°, 110°, and 130°). A sum of two exponentials was then fitted to the intensity correlation function and the decay rates were obtained from the fit. The results were in agreement with the TEM and viscosity results where large, multiparticle aggregates were observed for Disperbyk-170/-180 as well as the hydroxyl-terminated dendrimers. Intermediate sizes were observed for the phosphoric acid-terminated dendrimers and Disperbyk-111 while the smallest particle sizes were observed for the second generation, carboxylic acid-terminated dendrimer. In this case, the average particle size was observed to be approximately double the size of individual titania nanoparticles which correlates with a large percentage of stabilized single particles.

Dispersion Studies for Gold Nanoparticles

To assess the applicability of hybrid dendritic-linear dispersants to gold nanoparticles, citrate-stabilized gold particles of average diameter 12 nm were prepared in aqueous solution using the method of Turkevich et al.[26] A solution of the

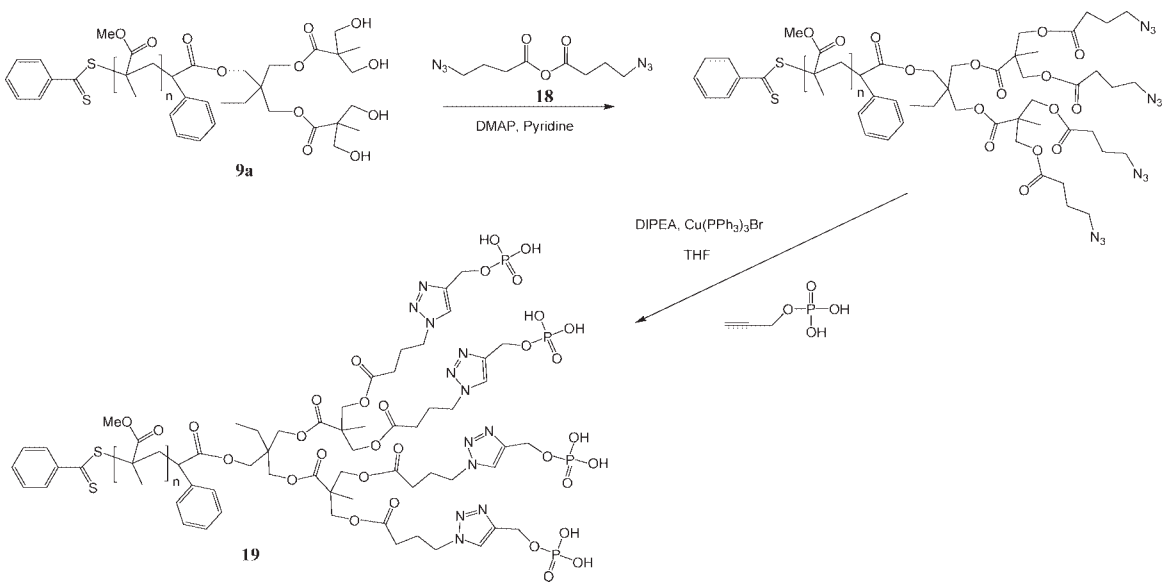

Scheme 9. Orthogonal synthesis of phosphonic acid functionalized dendritic dispersant, **19**.

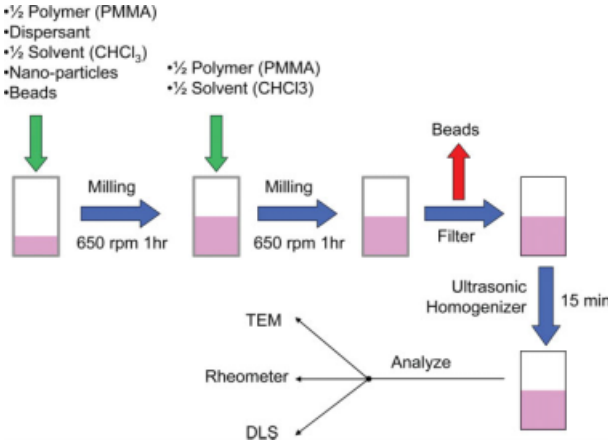

Figure 4. Procedure for milling experiments.

thioctic acid-functionalized hybrid dendritic-linear dispersant in tetrahydrofuran (7 mg dispersant in 2.5 mL of tetrahydrofuran) was added to a small sample of gold particles (1 mg gold in 5.5 g water) in a glass vial, with thorough mixing to ensure that the dispersant displaced the surface citrate groups of the Au nanoparticles. To demonstrate the efficient surface functionalization, the modified Au nanoparticles could be phase-transferred into the chloroform layer (Fig. 12) following the method of Merican et al.[27]

The organic soluble Au nanoparticles were then concentrated by centrifugation and the supernatant liquid (containing excess dispersant) removed. Significantly, the isolated solid Au nanoparticles could be redispersed in organic solvents and used for dispersion into a high molecular weight poly(methyl methacrylate) matrix (10 wt % of Au). The dispersion of the polymer-stabilized Au nanoparticles was examined by dropcasting on to a TEM grid. Significantly, the second-generation hybrid dendritic macromolecules were again observed to give optimal dispersion with thioctic acid end groups with little or no aggregation being observed (Fig. 13). Decreased levels of dispersion were observed for the first and third generation derivatives and no dispersion for dendrimers with hydroxyl or carboxylic acid ends. Analogous behavior was found for the phosphine oxide-terminated dendrimers and their ability to disperse CdSe nanoparticles in a high molecular weight PMMA matrix strongly suggesting that for nanoparticles of less than 20 nm in diameter an optimal size/number of chain ends groups for dispersion is approximately [G-2] for a 5 K polymeric tail.

CONCLUSIONS

The ability to accurately control molecular architecture has been used to prepare a library of hybrid dendritic-linear block copolymers based on a novel synthetic strategy using dendritic RAFT macroinitiators. This allows the degree of polymerization of the linear block, as well as the generation number of the dendrimer, to be controlled. This strategy coupled with the use of facile chain end modification chemistry permitted these novel dispersing agents to be tuned for a variety of

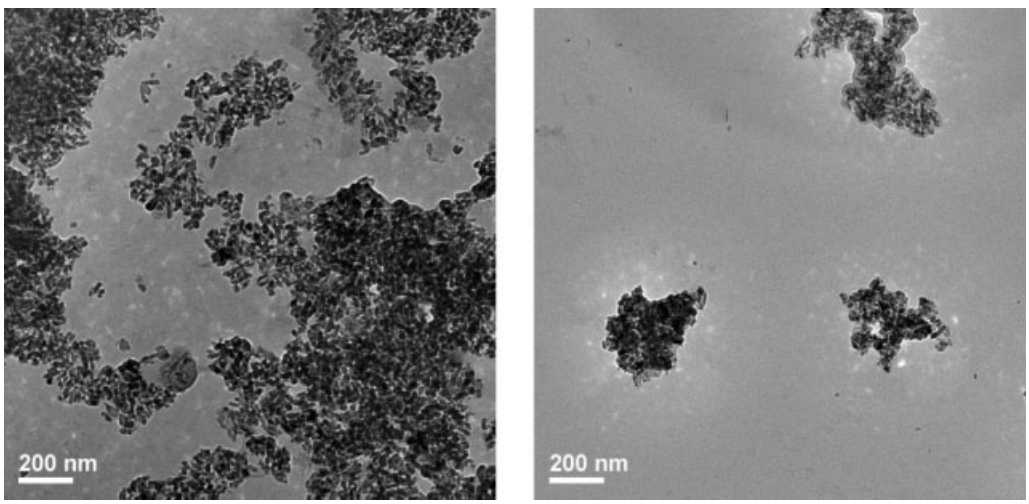

Figure 5. TEM images of composites formed by the dispersion of TiO_2 nanoparticles in a PMMA matrix with the addition of no dispersing agent. TTO-51(A) (left) and TTO-51N (right).

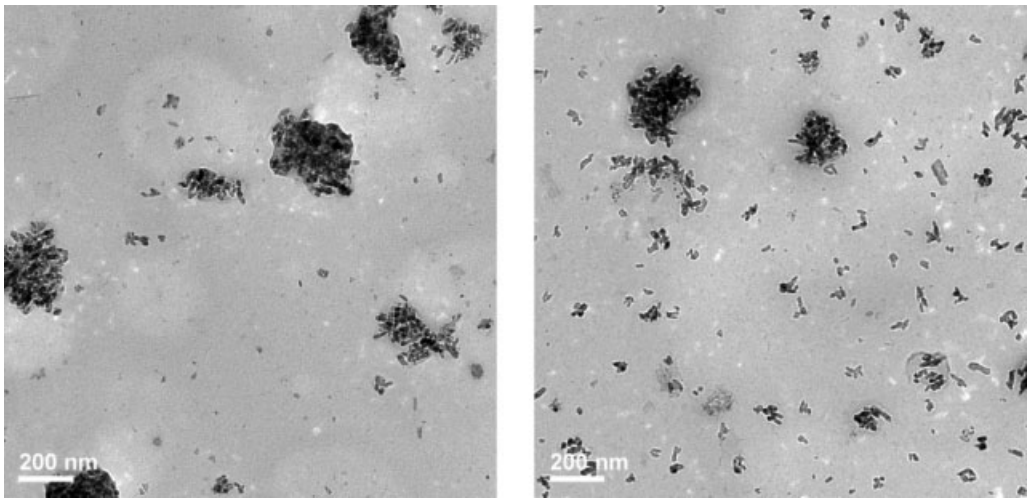

Figure 6. TEM images of composites formed by the dispersion of TiO_2 nanoparticles (TTO-51N) in a PMMA matrix with the addition of Disperbyk-170 (left) and Disperbyk-180 (right).

inorganic nanoparticles such as TiO_2, Au, and CdSe. For TiO_2, the optimal structure proved to be a second generation dendritic head group with carboxylic acid chain ends and dispersing agents based on these hybrid structures proved to be superior dispersing agents when compared to commercially available materials. Similar results were found for hybrid dendritic-linear dispersing agents containing disulphide (for Au) and phosphine oxide (for CdSe) chain ends and in each case uniform dispersion of discrete nanoparticles was observed in both solutions as well as in polymer matrices. These results demonstrate the power of well-defined macromolecular architectures to control interfacial interactions, critical in nanoparticle applications.

EXPERIMENTAL

General Methods

Analytical TLC was performed on commercial Merck Plates coated with silica gel GF254 (0.24 mm thick). Silica gel used for flash chromatography was Merck Kieselgel 60 (230–400 mesh, ASTM). ^{1}H NMR (400 MHz) and ^{13}C NMR (100 MHz) measurements were performed on a Bruker AC 200 spectrometer at room temperature. Size exclusion chromatography (SEC) was carried out at room temperature on a Waters chromatograph connected to a Waters 410 differential refractometer and six Waters Styragel® columns (five HR-5 μm and one HMW-20 μm) using THF as eluent

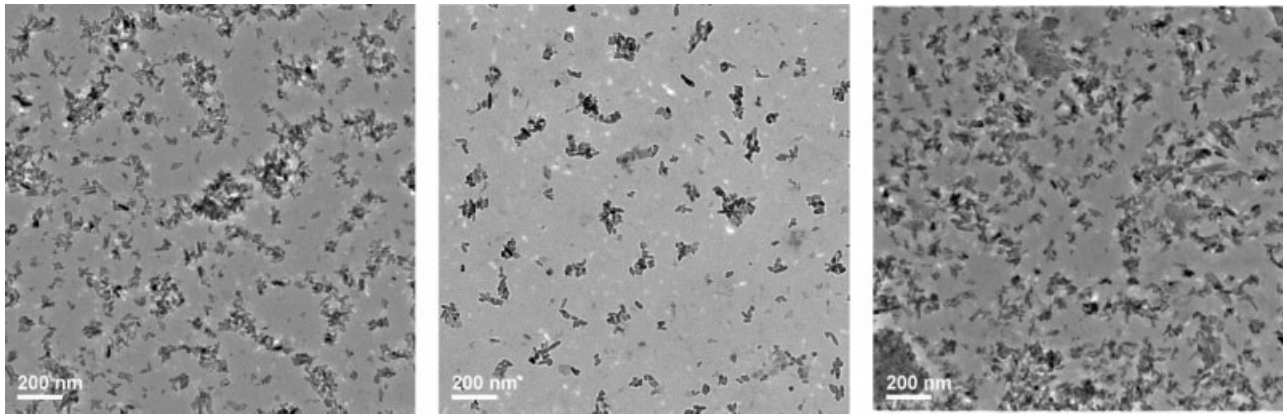

Figure 7. TEM images of composites formed by the dispersion of TiO_2 nanoparticles (TTO-51N) in a PMMA matrix with the addition of no different concentrations of Disperbyk-111, 10% (left), 5% (middle), and 2.5% (right).

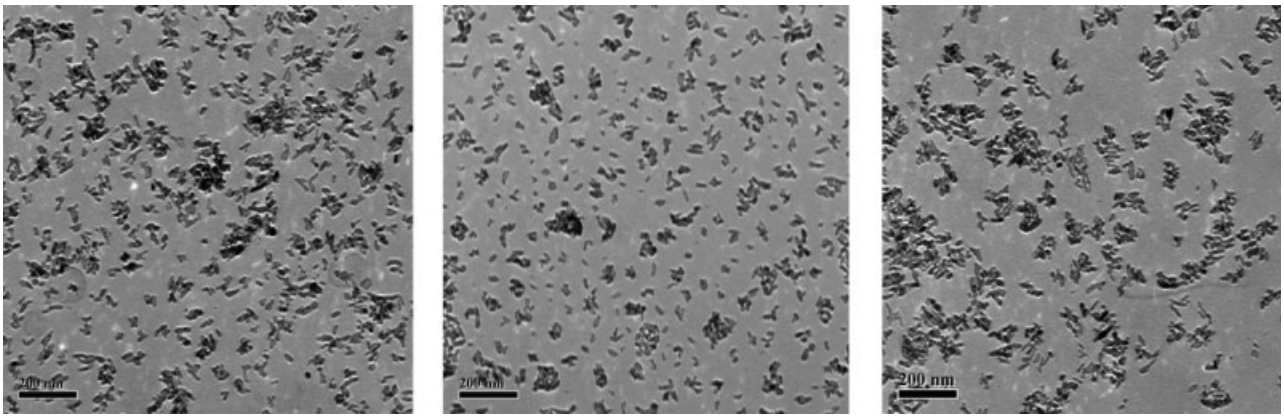

Figure 8. TEM images of composites formed by the dispersion of 20 wt % TiO_2 nanoparticles (TTO-51N) in a PMMA matrix with the addition of different generations of carboxylic functional dispersing agents: $(HOOC)_2$-G1-PMMA (left), $(HOOC)_4$-G2-PMMA (middle), and $(HOOC)_8$-G3-PMMA (right).

(flow rate: 1 mL/min). A Waters 410 differential refractometer and a 996 photodiode array detector were employed. The molecular weights of the polymers were calculated relative to linear polystyrene standards. The viscosity was measured with a TA ARES rheometer with a coquette test setup with 34 mm Ø cup and a 32 mm Ø bob of 33.3 mm. The experiments were run at 25 °C for 30 s at both clockwise and counter clockwise rotation speeds 1, 10 and 1/s. A low viscous silicon oil (DMS-T05, 5.00cSt) from Gelest Inc. was gently placed over the top of the sample to avoid evaporation of the solvent during measurement. Dynamic light scattering (DLS) analysis was carried out by BI-9000AT Digital autocorrelator with BI-APD Avalanche photodiode detector (Brookhaven Instruments Ltd., NY) equipped with 10 mW HeNe laser with power module. The samples were diluted to 0.5% of the original concentration for the DLS measurements to avoid multiple scattering effect. The intensity correlation functions were collected at five different angles (30°, 60°, 90°, 110°, and 130°). A sum of two exponentials was then fitted to the intensity correlation function and the decay rates were obtained from the fit. The decay rates are then plotted against the

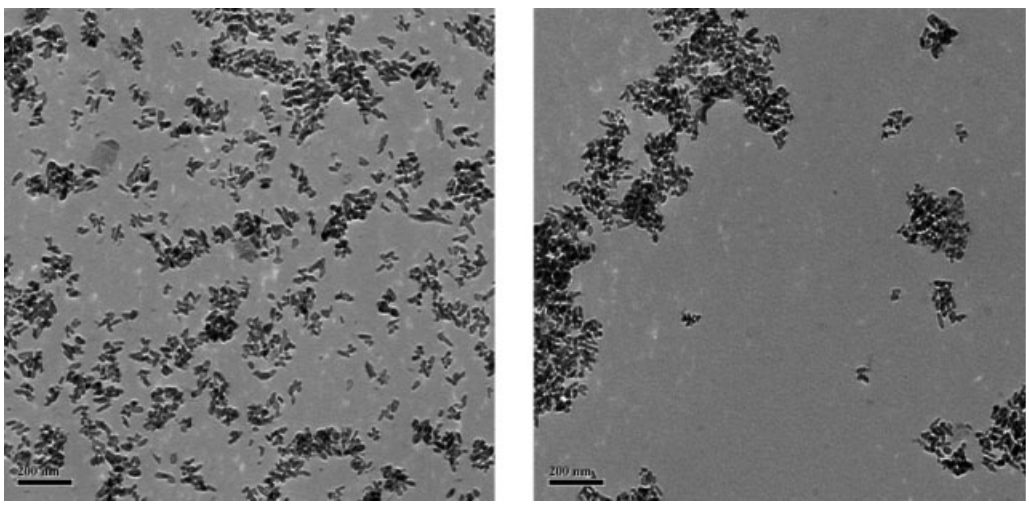

Figure 9. TEM images of composites formed by the dispersion of 20 wt % TiO_2 nanoparticles (TTO-51N) in a PMMA matrix with the addition of different generations of phosphoric acid functional dispersing agents: $(H_2PO_4)_4$-G2-PMMA (left) and $(H_2PO_4)_8$-G3-PMMA (right).

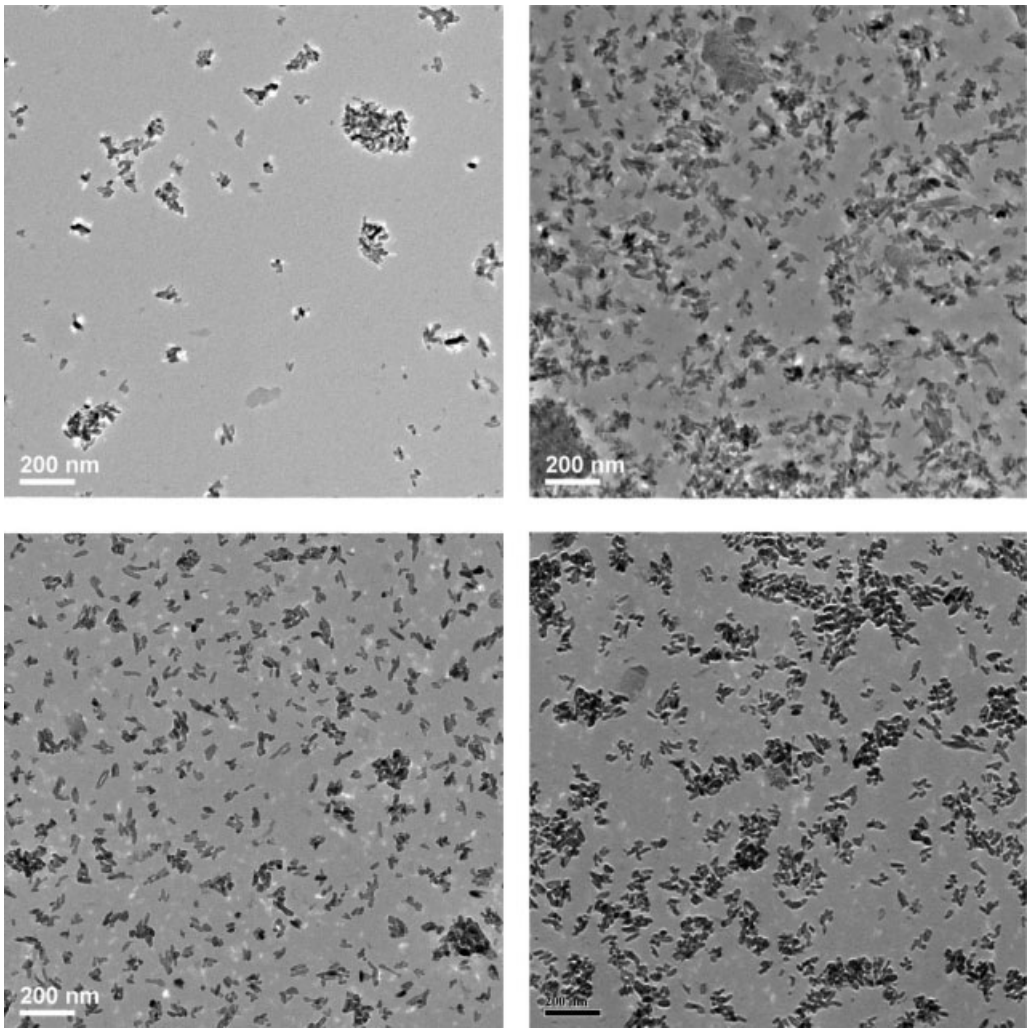

Figure 10. TEM images of composites formed by the dispersion of TiO_2 nanoparticles (TTO-51N) in a PMMA matrix with the addition of $(HO)_4$-G2-PMMA (top left), Disperbyk-111 (top right), $(HOOC)_4$-G2-PMMA (lower left), and $(H_2PO_4)_4$-G2-PMMA (lower right).

scattering vector, q. The data should all fit on a straight line and the slope of this line is the diffusion coefficient that can be used to calculate the hydrodynamic radius of the particles by the Stoke-Einstein equation. TEM samples were prepared by evaporating a drop of solution diluted to $\sim$ 5% onto a carbon-coated grid, and samples were analyzed on a FEI T20 at 200 keV.

Materials

$CuBr(PPh_3)_3$,[28] acetonide-protected bisMPA,[17] 4-(*N*,*N*-dimethylamino)pyridinium-*p*-toluenesulfonate (DPTS),[29] and 4-azidobutanoic acid[30] were synthesized according to previously described procedures. The nanoparticles (TTO-51(A), TTO-51N) were obtained from Ishihara Sangyo Kaisha Ltd. All other reagents were obtained from Aldrich and used as received.

Acetonide-2,2-bis(methylol) Propanol, 1

To a stirred solution of trimethylolpropane (TMP) (50.0 g, 373 mmol) in acetone (1000 mL), *p*-toluenesulfonic acid (*p*-TSA) (1.39 g, 7.46 mmol) and 2,2-dimethylolpropane (58.2 g, 560 mmol) were added. The reaction was stirred overnight and quenched with NH_4OH/ethanol (50/50 v/v) and the acetone evaporated. The crude product was dissolved in CH_2Cl_2 (1000 mL), extracted three

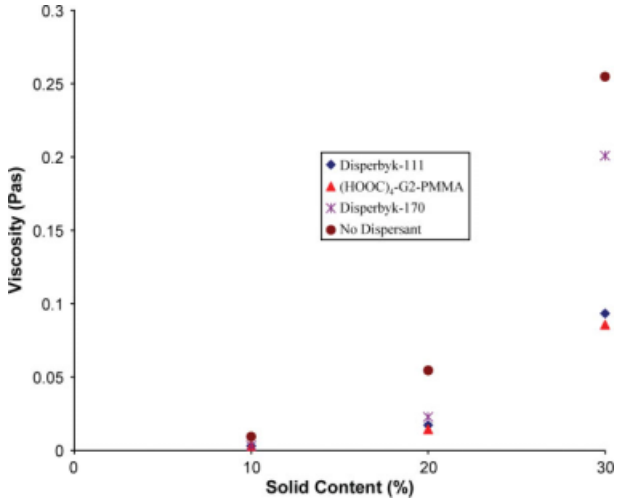

Figure 11. Relationship of viscosity with percent solid content for TiO_2 nanoparticles (TTO-51N) in the presence of various dispersing agents.

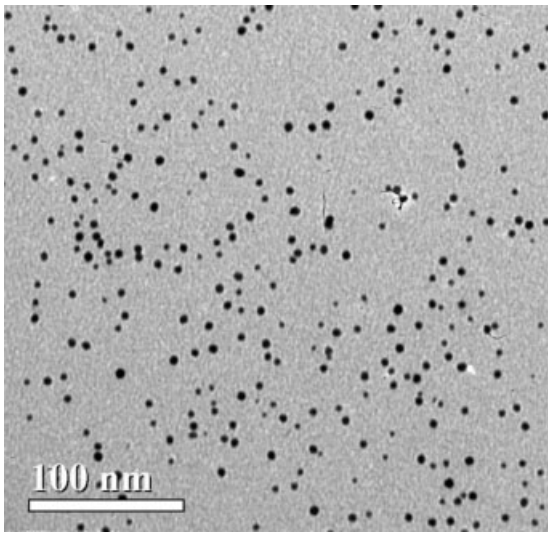

Figure 13. TEM of (thioctic)$_4$-G2-PMMA stabilized Au nanoparticles dispersed in a high molecular weight PMMA matrix (M_n = 150,000 Da).

times with water (100 mL), dried with $MgSO_4$, and concentrated to yield **1** as a colorless oil (56.5 g, 87%).

^{1}H NMR ($CDCl_3$): δ 0.79 (t, CH_2CH_3, J = 7.6 Hz, 3H), 1.30 (q, CH_2CH_3, J = 7.6 Hz, 2H), 1.38 (s, CCH_3, 3H), 1.41 (s, CCH_3, 3H), 2.70 (t, —OH, J = 7.4 Hz, 1H), 3.54 (s, CH_2OH, 2H), 3.65 (s, CH_2O, 2H), 3.68 (s, CH_2O, 2H). ^{13}C NMR ($CDCl_3$): δ 7.00 (s, CH_2CH_3, 1C), 20.17 (s, CH_2CH_3, 1C), 23.74 (s, CCH_3, 1C), 27.30 (s, CCH_3, 1C), 36.91 (s, $C(CH_2)_4$, 1C), 62.51 (s, CH_2OH, 1C), 65.15 (s, CH_2O, 2C), 98.16 (s, $C(CH_3)_2$, 1C).

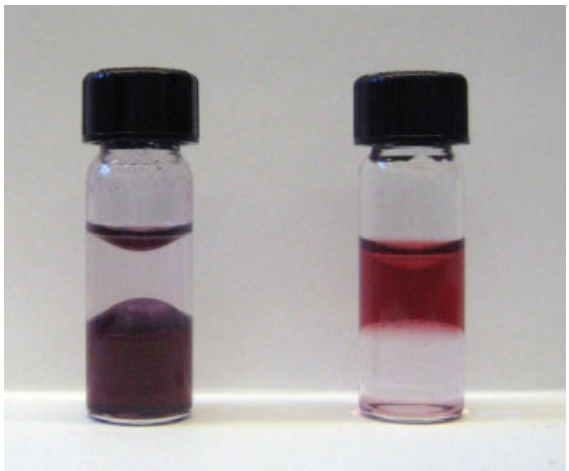

Figure 12. Phase transfer of citrate stabilized Au nanoparticles. Chloroform water mixtures with the dispersing agent (thioctic)$_4$-G2-PMMA (left) and without dispersing agent (right).

(Acetonide-2,2-bis(methylol) propyl)-2-bromo-2-phenylacetate, 3

To a solution of 2,2-bis(methylol) propanol (5.00 g, 28.7 mmol), α-bromophenylacetic acid (7.42 g, 34.5 mmol), and DPTS[23] (1.69 g, 5.70 mmol) in CH_2Cl_2 (25 mL), a solution of *N,N′*-dicyclohexylcarbodiimide (DCC) (8.90 g, 43.1 mmol) in CH_2Cl_2 (25 mL) was added dropwise. The reaction mixture was stirred at room temperature for 24 h, filtered, and the crude product purified by column chromatography, eluting from hexane to 10:90 ethyl acetate:hexane, to give the pure product, **3**, as a colorless oil (7.80 g, 73%).

^{1}H NMR ($CDCl_3$): δ 0.76 (t, CH_2CH_3, J = 7.6 Hz, 3H), 1.24 (q, CH_2CH_3, J = 7.6 Hz, 2H), 1.37 (s, CCH_3, 3H), 1.40 (s, CCH_3, 3H), 3.57 (s, CH_2O, 4H), 4.29 (s, CH_2OOC, 2H), 5.37 (s, Br-CHAr, 1H), 7.29–7.55 (m, *o,m,p*-ArH, 5H), ^{13}C NMR ($CDCl_3$): δ 6.91 (s, CH_2CH_3, 1C), 20.50 (s, CH_2CH_3, 1C), 23.81 (s, CCH_3, 1C), 26.88 (s, CCH_3, 1C), 36.22 (s, $C(CH_2)_4$, 1C), 46.95 (s, CHBr, 1C), 64.91 (s, CH_2O, 2C), 65.81 (s, CH_2OOC, 1C), 98.29 (s $C(CH_3)_2$, 1C), 128.65–129.31 (3s, ArC, 5C), 135.77(s, ArCCHBr, 1C), 168.06 (s, $COOCH_2$, 1C).

(Acetonide-2,2-bis(methylol) propyl)-2-phenyl-2-(phenylcarbonothioyl)thioacetate (Acetonide-G1-RAFT), 4

Carbon disulfide (5.00 mL, 82.8 mmol) was added dropwise to a solution of phenylmagnesium bromide (3.0 M in diethyl ether, 12.0 mL, 33.1 mmol) in 100 mL of dry tetrahydrofuran. The mixture was stirred at 50 °C to form a dark-brown solution and a solution of (2,2-bis(methylol) propyl)-2-bromo-2-phenylacetate (10.2 g, 27.6 mmol) in 20 mL of dry THF was then added. The reaction mixture was heated to 80 °C for 24 h, the solvent evaporated onto silica gel, and the crude product purified by column chromatography, eluting with hexane gradually increasing to 7.5:92.5 ethyl acetate:hexane, to give the generation 1, RAFT agent, **4**, as a red oil (6.80 g, 55%).

^{1}H NMR ($CDCl_3$): δ 0.74 (t, $CH_2C\mathbf{H_3}$, J = 7.6 Hz, 3H), 1.27 (q, $C\mathbf{H_2}CH_3$, J = 6.0 Hz, 2H), 1.36 (s, $CC\mathbf{H_3}$, 3H), 1.39 (s, $CC\mathbf{H_3}$, 3H), 3.61 (m, $C\mathbf{H_2}O$, 4H), 4.27 (m, $C\mathbf{H_2}COO$, 2H), 5.76 (s, PhC**H**, 1H), 7.27–7.50 (m, *m,p-Ar***H**CSS and *o*,m,*p*-Ar, 8H), 7.99 (dd, J = 7.4 Hz, *o-Ar***H**CSS, 2H). ^{13}C NMR ($CDCl_3$): ^{13}C NMR ($CDCl_3$): δ 7.01 (s, $CH_2\mathbf{C}H_3$, 1C), 21.11 (s, $\mathbf{C}H_2CH_3$, 1C), 23.85 (s, $C\mathbf{C}H_3$, 1C), 26.37 (s, $C\mathbf{C}H_3$, 1C), 36.24 (s, $\mathbf{C}(CH_2)_4$, 1C), 58.75 (s, **C**HSSCAr, 1C), 64.99 (s, $\mathbf{C}H_2O$, 2C), 65.67 (s, $\mathbf{C}H_2OOC$, 1C), 98.28 (s $C(CH_3)_2$, 1C), 126.98–132.88 (6s, Ar**C**, 10C), 133.51 (s, Ar**C**CHS, 1C), 144.01 (s, Ar**C**CSS, 1C), 168.78 (s, **C**$OOCH_2$, 1C).

General Procedure for Deprotection of Acetonide Protecting Groups, 2,2-bis(methylol) propyl)-2-phenyl-2-(phenylcarbonothioyl)thioacetate $(HO)_2$-G1-RAFT, 5

To a stirred solution of acetonide-G1-RAFT (5.00 g, 11.2 mmol) in 300 mL of MeOH was added DOWEX, 50 × 200 resin (10.0 g). The reaction was stirred at 50 °C for 8 h, the resin was filtered, and the organic phase concentrated to give **5** as a red oil, which was essentially pure and did not require further purification (4.13 g, 91%).

^{1}H NMR ($CDCl_3$): δ 0.84 (t, $CH_2C\mathbf{H_3}$, J = 6.4 Hz, 3H), 1.22 (q, $C\mathbf{H_2}CH_3$, J = 7.0 Hz, 2H), 3.24 (t, O**H**, J = 7.0 Hz, 2H), 3.51 (m, $C\mathbf{H_2}OH$, 4H), 4.19 (q, $C\mathbf{H_2}OOC$, J = 7.0 Hz, 2H), 5.74 (s, PhC**H**, 1H), 7.27–7.52 (m, *m,p-Ar***H**CSS and *o*,m,*p*-Ar, 8H) 7.98 (dd, J = 7.2 Hz, *o-Ar***H**CSS, 2H). ^{13}C NMR ($CDCl_3$): ^{13}C NMR ($CDCl_3$): δ 7.30 (s, $CH_2\mathbf{C}H_3$, 1C), 22.18 (s, $\mathbf{C}H_2CH_3$, 1C), 29.67 (s, $\mathbf{C}(CH_2)_4$, 1C), 58.96 (s, **C**HSSCAr, 1C), 64.88 (s, $\mathbf{C}H_2OH$, 2C), 65.92 (s, $\mathbf{C}H_2OOC$, 1C), 126.88–132.94 (6s, Ar**C**, 10C), 133.03 (s, Ar**C**CHS, 1C), 143.76 (s, Ar**C**CSS, 1C), 169.56 (s, **C**$OOCH_2$, 1C).

General Procedure for Dendritic Growth with Acetonide Protected Acetonide-2,2-bis(methoxy) Propionic Acid, Acetonide-G2-RAFT, 7

To a stirred solution of $(HO)_2$-G1-RAFT (0.60 g, 1.48 mmol), DMAP (72 mg, 0.59 mmol, 0.2 eq/OH), and pyridine (11.7 g, 14.8 mmol, 5 eq/OH) in CH_2Cl_2 (10 mL), acetonide-2,2-bis(methoxy)propanoic anhydride (1.47 g, 4.45 mmol, 1.5 eq/OH) was added and the reaction mixture stirred overnight at room temperature under argon. The residual anhydride was quenched by reaction with ~ 10 mL of water under rigorous stirring for 2 h. The reaction mixture was then taken up into ~ 150 mL of dichloromethane and extracted three times with $NaHSO_4$ (50 mL), three times with of $NaHCO_3$ (50 mL), and finally once with brine (50 mL). The organic layer was dried with $MgSO_4$, the solvent was evaporated, and the crude product was purified by flash chromatography eluting with hexane gradually increasing to 25/75 ethyl acetate/hexane to give the second generation derivative, **7**, as a red sticky solid (0.94 g, 89%).

^{1}H NMR ($CDCl_3$): δ 0.83 (t, $CH_2C\mathbf{H_3}$, J = 6.2 Hz, 3H), 1.10 (s, $CC\mathbf{H_3}$, 6H), 1.32 (s, $CC\mathbf{H_3}$, 6H), 1.39 (s, $CC\mathbf{H_3}$, 6H), 1.44 (q, $C\mathbf{H_2}CH_3$, J = 6.0 Hz, 2H), 3.59 (m, $C\mathbf{H_2}O$, 4H), 4.27 (m, $C\mathbf{H_2}COO$, 2H, $C\mathbf{H_2}O$, 4H, and $C\mathbf{H_2}O$, 4H), 5.69 (s, PhC**H**, 1H), 7.29–7.50 (m, *m,p-Ar***H**CSS and *o*,m,*p*-Ar, 8H), 7.97 (dd, J = 7.0 Hz, *o-Ar***H**CSS, 2H). ^{13}C NMR ($CDCl_3$): δ 7.31 (s, $CH_2\mathbf{C}H_3$, 1C), 18.27 (s, $C\mathbf{C}H_3$, 2C), 21.18 (s, $\mathbf{C}H_2CH_3$, 1C), 23.23 (s, $C\mathbf{C}H_3$, 2C), 26.07 (s, $C\mathbf{C}H_3$, 2C), 41.58 (s, $\mathbf{C}(CH_2)_4$, 1C), 42.16 (s, $\mathbf{C}CH_2O$, 2C), 58.82 (s, **C**HSSCAr, 1C), 63.18 (s, $\mathbf{C}H_2O$, 2C), 64.83 (s, $C\mathbf{C}H_2OH$, 4C), 65.93 (s, $\mathbf{C}H_2OOC$, 1C), 98.13 (s $C(CH_3)_2$, 1C), 126.85–132.94 (6s, Ar**C**, 10C), 132.94 (s, Ar**C**CHS, 1C), 143.77 (s, Ar**C**CSS, 1C), 168.26 (s, **C**$OOCH_2$, 1C), 174.12 (s, **C**OO, 2C).

$(HO)_4$-G2-RAFT, 20

Following a similar procedure as for $(HO)_2$-G1-RAFT, **5**, the second generation derivative, **20**, was obtained as a red sticky solid (87%).

^{1}H NMR (MeOD): δ 0.83 (t, $CH_2C\mathbf{H_3}$, J = 7.6 Hz, 3H), 1.08 (s, $CC\mathbf{H_3}$, 6H), 1.42 (q, $C\mathbf{H_2}CH_3$, J = 7.2 Hz, 2H), 3.22 (s, O**H**, J = 7.0 Hz, 4H), 4.27 (m, $C\mathbf{H_2}COO$, 2H, and $C\mathbf{H_2}O$, 4H), 5.73 (s, PhC**H**, 1H), 7.20–7.55 (m, *m,p-Ar***H**CSS and *o*,m,*p*-Ar, 8H), 7.96 (dd, J = 7.4 Hz, *o-Ar***H**CSS, 2H). ^{13}C

NMR (MeOD): δ 6.45 (s, $CH_2\mathbf{C}H_3$, 1C), 16.13 (s, $C\mathbf{C}H_3$, 2C), 22.46 (s, $\mathbf{C}H_2CH_3$, 1C), 41.31 (s, $\mathbf{C}(CH_2)_4$, 1C), 50.31 (s, $\mathbf{C}CH_2OH$, 2C) 58.88 (s, **C**HSSCAr, 1C), 63.04 (s, $\mathbf{C}H_2O$, 2C), 64.48 (s, $C\mathbf{C}H_2OH$, 4C), 64.79 (s, $\mathbf{C}H_2OOC$, 1C), 126.56–129.05 (6s, Ar**C**, 10C), 132.96 (s, Ar**C**CHS, 1C), 143.87 (s, Ar**C**CSS, 1C), 168.49 (s, $\mathbf{C}OOCH_2$, 1C), 174.70 (s, **C**OO, 2C).

Acetonide-G3-RAFT, 6

Purified by flash chromatography using hexane gradually increasing to 40/60 ethyl acetate/hexane giving **6** as a red solid (88%).

^{1}H NMR ($CDCl_3$): δ 0.82 (t, $CH_2C\mathbf{H_3}$, J = 6.2 Hz, 3H), 1.12 (s, $CC\mathbf{H_3}$, 12H), 1.34 (s, $CC\mathbf{H_3}$, 12H), 1.40 (s, $CC\mathbf{H_3}$, 12H), 1.45 (q, $C\mathbf{H_2}CH_3$, J = 6.0 Hz, 2H), 3.58 (m, $C\mathbf{H_2}O$, 8H), 4.00–4.30 (m, $C\mathbf{H_2}COO$, 2H, $C\mathbf{H_2}O$, 4H, $C\mathbf{H_2}O$, 8H and $C\mathbf{H_2}O$, 8H), 5.68 (s, PhC**H**, 1H), 7.30–7.50 (m, *m,p-Ar***H**CSS and *o*,m,*p*-Ar, 8H), 7.99 (dd, J = 7.0 Hz, *o-Ar***H**CSS, 2H). ^{13}C NMR ($CDCl_3$): δ 7.44 (s, $CH_2\mathbf{C}H_3$, 1C), 17.83 (s, $C\mathbf{C}H_3$, 2C), 18.62 (s, $C\mathbf{C}H_3$, 4C), 21.23 (s, $\mathbf{C}H_2CH_3$, 1C), 22.12 (s, $C\mathbf{C}H_3$, 4C), 25.36 (s, $C\mathbf{C}H_3$, 4C), 41.58 (s, $\mathbf{C}(CH_2)_4$, 1C), 42.16 (s, $\mathbf{C}CH_2O$, 4C), 47.03 (s, $\mathbf{C}CH_2O$, 2C), 58.93 (s, **C**HSSCAr, 1C), 63.98 (s, $\mathbf{C}H_2O$, 2C), 64.94 (s, $C\mathbf{C}H_2OH$, 4C), 66.05 (s, $C\mathbf{C}H_2OH$, 8C) 66.11 (s, $\mathbf{C}H_2OOC$, 1C), 98.23 (s $C(CH_3)_2$, 1C), 127.08–129.35 (6s, Ar**C**, 10C), 133.08 (s, Ar**C**CHS, 1C), 143.93 (s, Ar**C**CSS, 1C), 168.29 (s, $\mathbf{C}OOCH_2$, 1C), 172.09 (s, **C**OO, 2C), 173.61 (s, **C**OO, 4C).

General Procedure for Polymerization, Exemplified with Acetonide-G1-PMMA, 21

Acetonide-G1-RAFT, **4** (890 mg, 2.00 mmol), AIBN (33 mg, 0.20 mmol) was dissolved in neat MMA (5.00 g, 49.9 mmol) in a glass tube. The tube was degassed by freeze-pump-thaw cycles and sealed off under vacuum. The polymerization was run at 70 °C for 2 h and then cooled. The crude polymer was purified by MPLC using hexane gradually increasing to ethyl acetate giving **21** as a pink solid. Conversion was evaluated by ^{1}H NMR of the crude polymer solution, and the molecular weight and polydispersity index were determined by SEC (yield = 67%, M_n = 5000 g/mol, PDI = 1.21).

^{1}H NMR δ 0.55 (t, $CH_2C\mathbf{H_3}$) 0.8–2.1 (broad m, PMMA C**H**, CH_2, $C\mathbf{H_3}$), 1.11 (s, $CC\mathbf{H_3}$)1.32 (s, $CC\mathbf{H_3}$), 3.1–3.8 (broad m, $C\mathbf{H_2}O$, PMMA $OC\mathbf{H_3}$), 3.9–4.1 ($C\mathbf{H_2}COO$), 7.25–7.50 (m, *m,p-Ar***H**CSS and *o*,m,*p*-Ar), 8.0 (dd, J = 7.4 Hz, *o-Ar***H**CSS) ^{13}C NMR ($CDCl_3$): δ 7.12, 16.34, 18.35, 21.03, 42.10, 44.43, 44.78, 45.43, 51.77, 52.67, 54.28, 60.31, 64.27, 65.93, 97.98, 126.62, 128.28, 173.52, 176.90, 177.75, 178.33.

Acetonide-G2-PMMA, 8

Following a similar procedure as for acetonide-G1-RAFT, **21**, the second generation derivative, **8**, was obtained as a pink solid.

^{1}H NMR ($CDCl_3$) δ 0.7–2.1 (broad m, PMMA C**H**, CH_2, $C\mathbf{H_3}$), 1.11 (s, $CC\mathbf{H_3}$)1.32 (s, $CC\mathbf{H_3}$), 3.1–3.8 (broad m, $C\mathbf{H_2}O$, PMMA $OC\mathbf{H_3}$), 3.9–4.1 (m, $C\mathbf{H_2}COO$ and $C\mathbf{H_2}O$), 7.25–7.50 (m, *m,p-Ar***H**CSS and *o*,m,*p*-Ar), 8.0 (dd, J = 7.4 Hz, *o-Ar***H**CSS). ^{13}C NMR ($CDCl_3$): δ 7.09, 14.15, 16.32, 18.35, 21.00, 42.00, 44.43, 44.78, 45.43, 51.77, 52.67, 54.28, 60.31, 64.27, 65.93, 97.98, 126.62, 128.28, 173.52, 176.90, 177.75, 178.33.

Acetonide-G3-PMMA, 22

Following a similar procedure as for acetonide-G1-RAFT, **21**, the third generation derivative, **22**, was obtained as a pink solid.

^{1}H NMR ($CDCl_3$) δ 0.7–2.1 (broad m, PMMA C**H**, CH_2, $C\mathbf{H_3}$), 1.12 (s, $CC\mathbf{H_3}$), 1.34 (s, $CC\mathbf{H_3}$), 3.1–3.8 (broad m, $C\mathbf{H_2}O$, PMMA $OC\mathbf{H_3}$), 3.9–4.1 (m, $C\mathbf{H_2}COO$, and $C\mathbf{H_2}O$), 7.25–7.50 (m, *m,p-Ar***H**CSS and *o*,m,*p*-Ar), 8.0 (dd, J = 7.4 Hz, *o-Ar***H**CSS). ^{13}C NMR ($CDCl_3$): δ 7.13, 14.14, 17.06, 17.58, 18.38, 20.99, 21.84, 25.25, 30.88,41.95, 42.10, 44.41, 45.41, 46.77, 54.31, 60.29, 64.67, 65,88, 98.13, 126.60, 128.27, 144.73, 173.39, 177.03, 177.77, 178.02.

Acetonide-G4-PMMA, 23

Following a similar procedure as for acetonide-G1-RAFT, **21**, the fourth generation derivative, **23**, was obtained as a pink solid.

^{1}H NMR ($CDCl_3$) δ 0.7–2.1 (broad m, PMMA C**H**, CH_2, $C\mathbf{H_3}$), 1.10 (s, $CC\mathbf{H_3}$), 1.33 (s, $CC\mathbf{H_3}$), 3.1–3.8 (broad m, $C\mathbf{H_2}O$, PMMA $OC\mathbf{H_3}$), 3.9–4.1 (m, $C\mathbf{H_2}COO$, and $C\mathbf{H_2}O$), 7.25–7.50 (m, *m,p-Ar***H**CSS and *o*,m,*p*-Ar), 8.0 (dd, J = 7.4 Hz, *o-Ar***H**CSS). ^{13}C NMR ($CDCl_3$): δ 7.11, 14.12, 17.06, 17.42, 17.93, 18.48, 20.87, 21.82, 25.25, 30.78, 41.92, 42.10, 44.39, 45.41, 54.31, 60.29, 64.69, 65.72, 98.16, 126.63, 128.27, 144.73, 173.39, 174.32, 177.03, 177.73, 178.32.

$(HO)_2$-G1-PMMA, 24

Acetonides were deprotected according to general deprotection procedure except that the polymer was dissolved in THF and sufficient MeOH added to maintain solubility without precipitating the polymer. The product was a pink solid (95%).

^{1}H NMR δ 0.8–2.1 (broad m, PMMA C**H**, CH_2, C**H$_3$**), 3.1–3.8 (broad m, PMMA OC**H$_3$**), 3.9–4.1 (m, C**H$_2$**OH, C**H$_2$**COO), 7.25–7.50 (m, *m,p-Ar***H**CSS and *o*,m,*p*-Ar), 8.0 (dd, J = 7.4 Hz, *o-Ar***H**CSS) ^{13}C NMR ($CDCl_3$): δ 7.12, 16.38, 18.69, 21.02, 44.50, 44.84, 45.49, 51.82, 52.86, 54.38, 62.76, 126.68, 128.32, 128.74, 176.97, 177.81, 178.10.

$(HO)_4$-G2-PMMA, 9a

Following a similar procedure as for $(HO)_2$-G1-PMMA, **24**, the second generation derivative, **9a**, was obtained as a pink solid.

^{1}H NMR ($CDCl_3$) δ 0.8–2.1 (broad m, PMMA C**H**, CH_2, C**H$_3$**), 3.1–3.8 (broad m, PMMA OC**H$_3$**), 3.9–4.1 (C**H$_2$**OH, C**H$_2$**COO, and C**H$_2$**O), 7.25–7.50 (m, *m,p-Ar***H**CSS and *o*,m,*p*-Ar), 8.0 (dd, J = 7.4 Hz, *o-Ar***H**CSS) ^{13}C NMR ($CDCl_3$): δ 7.01, 16.32, 17.08, 18.64, 26.68, 30.01, 44.46, 44.81, 45.46, 49.72, 51.80, 52.83, 54.31, 58.54, 62.63, 67.68, 72.73, 126.65, 128.30, 175.14, 176.94, 177.79, 178.08, 178.36.

$(HO)_8$-G3-PMMA, 25

Following a similar procedure as for $(HO)_2$-G1-PMMA, **24**, the third generation derivative, **25**, was obtained as a pink solid.

^{1}H ($CDCl_3$) NMR δ 0.8–2.1 (broad m, PMMA C**H**, CH_2, C**H$_3$**), 3.1–3.8 (broad m, PMMA OC**H$_3$**), 3.9–4.1 (m, C**H$_2$**OH, C**H$_2$**COO, and C**H$_2$**O), 7.25–7.50 (m, *m,p-Ar***H**CSS and *o*,m,*p*-Ar), 8.0 (dd, J = 7.4 Hz, *o-Ar***H**CSS) ^{13}C NMR ($CDCl_3$): δ 7.21, 16.33, 17.08, 17.94, 18.64, 20.98, 26.62, 29.97, 44.45, 44.80, 45.45, 46.51, 49.83, 51.80, 52.70, 54.35, 58.53, 58.90, 62.57, 64.69, 66.61, 72.72, 126.64, 127.67, 128.29, 132.48, 144.77, 172.46, 174.91, 176.93, 177.09, 178.08, 178.36.

General Procedure for Functionalizing with Carboxylic Acids, Exemplified with $(HOOC)_2$-G1-PMMA, 26

To a stirred solution of $(HO)_2$-G1-PMMA, **24** (1.45 g, 0.29 mmol), DMAP (14 mg, 0.06 mmol, 0.2 eq/OH), and pyridine (0.23 g, 2.90 mmol, 5 eq/OH) in 10 mL of CH_2Cl_2, succinic anhydride (0.29 g, 2.90 mmol, 5 eq/OH) was added. The reaction was stirred overnight at RT. The residual anhydride was quenched by reaction with $\sim$ 10 mL of water under vigorous stirring for a 2 h. The reaction mixture was then taken up into $\sim$ 150 mL of dichloromethane and extracted three times with $NaHSO_4$ (50 mL) and three times with brine (50 mL). The organic layer was dried with $MgSO_4$, the solvent was evaporated, and the crude product was dissolved in a small amount of CH_2Cl_2, precipitated into hexane, filtered, and dried to yield the **26** as a pink solid (94%).

^{1}H NMR ($CDCl_3$) δ 0.8–2.1 (broad m, PMMA C**H**, CH_2, C**H$_3$**), 2.3–2.5 (broad s, C**H$_2$**C**H$_2$**COOH) 3.1–3.8 (broad m, PMMA OC**H$_3$**), 3.9–4.1 (m, C**H$_2$**O, C**H$_2$**COO), 7.25–7.50 (m, *m,p-Ar***H**CSS and *o*,m,*p*-Ar), 8.0 (dd, J = 7.4 Hz, *o-Ar***H**CSS) ^{13}C NMR ($CDCl_3$): δ 11.42, 14.11, 16.37, 18.68, 20.68, 22.63, 25.25, 29.03, 31.56, 34.49, 34.63, 44.49, 44.83, 45.48, 51.81, 52.70, 54.37, 126.66, 128.31, 176.95, 177.81, 178.09.

$(HOOC)_4$-G2-PMMA, 10a

Following a similar procedure as for $(HOOC)_2$-G1-PMMA, **26**, the second generation derivative, **10a**, was obtained as a pink solid.

^{1}H NMR ($CDCl_3$) δ 0.8–2.1 (broad m, PMMA C**H**, CH_2, C**H$_3$**), 2.3–2.5 (broad s, C**H$_2$**C**H$_2$**COOH) 3.1–3.8 (broad m, PMMA OC**H$_3$**), 3.9–4.1 (m, C**H$_2$**O, C**H$_2$**COO), 7.25–7.50 (m, *m,p-Ar***H**CSS and *o*,m,*p*-Ar), 8.0 (dd, J = 7.4 Hz, *o-Ar***H**CSS). ^{13}C NMR ($CDCl_3$): δ 11.42, 14.11, 14.31, 16.36, 18.74, 16.36, 18.74, 20.43, 20.68, 22.64, 25.25, 28.83, 31.57, 34.64, 36.05, 41.32, 44.51, 44.85, 46.46, 51.81, 52.71, 54.40, 126.68, 128.32, 171.37, 176.97, 177.81, 178.10.

$(HOOC)_8$-G3-PMMA, 27

Following a similar procedure as for $(HOOC)_2$-G1-PMMA, **24**, the second generation derivative, **27**, was obtained as a pink solid.

^{1}H NMR ($CDCl_3$) δ 0.8–2.1 (broad m, PMMA C**H**, CH_2, C**H$_3$**), 2.3–2.5 (broad s, C**H$_2$**C**H$_2$**COOH) 3.1–3.8 (broad m, PMMA OC**H$_3$**), 3.9–4.1 (m, C**H$_2$**O, C**H$_2$**COO), 7.25–7.50 (m, *m,p-Ar***H**CSS and *o*,m,*p*-Ar), 8.0 (dd, J = 7.4 Hz, *o-Ar***H**CSS). ^{13}C NMR ($CDCl_3$): δ 11.45, 14.13, 16.43, 17.58, 18.70, 20.70, 22.60, 25.27, 28.85, 29.05, 31.59, 34.66, 44.52, 44.86, 46.47, 51.84, 54.33, 128.34, 171.61, 171.99, 177.01, 177.43, 177.33, 178.12.

Thioctic Anhydride, 11

To a stirred solution of thioctic acid (5.00 g, 24.2 mmol) in dichloromethane (25 mL), 1,3-dicyclohexylcarbodiimide (DCC) (2.50 g, 12.1 mmol) was added. The reaction mixture was stirred at room temperature overnight, filtered, and evaporated to dryness. After evaporation, the product, **11**, was obtained as a yellow solid (4.7 g, 98%).

^{1}H NMR ($CDCl_3$): δ 1.1–2.0 (broad m, C**H**$_2$CH$_2$COO, C**H**$_2$CH$_2$CH$_2$COO, C**H**$_2$CHSS, C**H**$_2$CH$_2$SS, 14HH), 2.3–2.5 (m, CH$_2$C**H**$_2$COO C**H**$_2$CH$_2$SS, 6H), 3.0–3.3 (m, CH$_2$C**H**$_2$SS, 4H), 3.5 (m, C**H**SS, 2H). ^{13}C NMR ($CDCl_3$). δ 23.92 (s, **C**H$_2$ CH$_2$COO, 2C), 28.45 (s, **C**H$_2$ CH$_2$CH$_2$COO, 2C), 34.57 (s, CH$_2$**C**H$_2$COO, 2C), 35.10 (s, **C**H$_2$CHSS, 2C), 38.50 (s, CH$_2$ **C**H$_2$SS, 2C), 40.22 (s, **C**H$_2$ CH$_2$SS, 2C), 56.21 (s, **C**HSS, 2C), 169.21 (s, **C**OO, 2C).

(Thioctic)$_4$-G2-PMMA, 12

To a stirred solution of (HO)$_4$-G2-PMMA, **9a** (1.00 g, 0.20 mmol), DMAP (20 mg, 0.08 mmol, 0.2 eq/OH), and pyridine (0.32 g, 4.00 mmol, 5 eq/OH) in 10 mL of CH_2Cl_2, thioctic anhydride, **11** (1.58 g, 4.00 mmol, 5 eq/OH) was added. The reaction was stirred overnight at RT. The residual anhydride was quenched by reaction with $\sim$ 10 mL of water under vigorous stirring for 2 h. The reaction mixture was then taken up into $\sim$ 150 mL of dichloromethane and extracted three times with $NaHSO_4$ (50 mL) and three times with brine (50 mL). The organic layer was dried with $MgSO_4$, the solvent was evaporated, and the crude product was purified by flash chromatography eluting with 60/40 ethyl acetate/hexane gradually increasing to ethyl acetate, concentrated, dissolved in a small amount of CH_2Cl_2, precipitated into hexane, filtered, and dried to yield **12** as a white solid (87%).

^{1}H NMR ($CDCl_3$) δ 0.8–2.1 (broad m, PMMA C**H**, CH$_2$, C**H**$_3$, broad m, C**H**$_2$CH$_2$COO, C**H**$_2$CH$_2$CH$_2$COO, C**H**$_2$CHSS, C**H**$_2$CH$_2$SS), 2.3–2.5 (broad m, CH$_2$C**H**$_2$COO C**H**$_2$CH$_2$SS) 3.1–3.8 (broad m, PMMA OC**H**$_3$, CH$_2$C**H**$_2$SS, C**H**SS), 3.9–4.1 (m, C**H**$_2$O, C**H**$_2$COO). ^{13}C NMR ($CDCl_3$): δ 11.42, 14.11, 16.42, 18.75, 22.64, 24.55, 25.27, 28.71, 29.05, 31.57, 34.65, 38.49, 40.24, 44.53, 44.88, 51.80, 54.45, 56.32, 172.43, 176.96, 177.78.

5-(Dioctylphosphoryl)pentanoic acid, 15

Di-*n*-octyl phosphine oxide (5.00 g, 18.2 mmol), 4-pentenoic acid (2.28 g, 22.8 mmol, 1.25 eq.), and AIBN (0.75 g, 4.6 mmol, 0.25 eq.) were mixed and deoxygenated by three freeze pump thaw cycles. The reaction was stirred under Ar over night at 80 °C. The crude product was purified with flash chromatography eluting with ethyl acetate increasing to 5/95 methanol/ethyl acetate, concentrated and followed by flash chromatography eluting with chloroform gradually increasing to 10/90 methanol/chloroform. The crude product was obtained as colorless oil (3.76 g, 55%).

^{1}H NMR ($CDCl_3$): δ 0.89 (t, J = 6.6 Hz, C**H**$_3$, 6H), 1.25–1.90 (broad m, octyl C**H**$_2$, PC**H**$_2$CH$_2$ and PCH$_2$C**H**$_2$, 32H), 2.34 (t, J = 6.0 Hz, C**H**$_2$COO, 2H). ^{13}C NMR ($CDCl_3$): δ 14.08, 21.07, 21.57, 22.62, 26.50, 26.74, 27.82, 28.04, 29.05, 30.93, 31.21, 31.78, 33.83, 175.56. ^{31}P NMR ($CDCl_3$): δ 52.88.

5-(Dioctylphosphoryl)pentanoic Anhydride, 13

To a stirred solution of 5-(dioctylphosphoryl)pentanoic acid, **15** (3.76 g, 10.1 mmol) in dichloromethane (20 mL), 1,3-dicyclohexylcarbodiimide (DCC) (1.04 g, 5.05 mmol) was added. The reaction mixture was stirred at room temperature over night, filtered, and evaporated to dryness. The byproducts were isolated through precipitation into ether (20 mL) and filtration. After evaporation, **13** was obtained as a yellow solid (3.19 g, 87%).

^{1}H NMR ($CDCl_3$): δ 0.92 (t, J = 6.4 Hz, C**H**$_3$, 12H), 1.20–1.95 (broad m, octyl C**H**$_2$, PC**H**$_2$CH$_2$ and PCH$_2$C**H**$_2$, 64H), 2.51 (t, J = 6.8 Hz, C**H**$_2$COO, 4H). ^{13}C NMR ($CDCl_3$): δ 14.05, 21.08, 21.74, 22.58, 25.41, 27.37, 28.26, 28.66, 29.06, 31.00, 31.75, 34.67, 34.89, 168.86. ^{31}P NMR ($CDCl_3$): δ 48.11.

(Phosphine oxide)$_4$-G2-PMMA, 16

To a stirred solution of (HO)$_4$-G2-PMMA (0.5 g, 0.10 mmol), DMAP (2 mg, 0.04 mmol, 0.2 eq/OH), and pyridine (0.16 g, 2.0 mmol, 5 eq/OH) in 10 mL of CH_2Cl_2, 5-(dioctylphosphoryl)pentanoic anhydride, **13** (1.46 g, 2.00 mmol, 5 eq/OH) was added. The reaction was stirred overnight at RT. The residual anhydride was quenched by reaction with $\sim$ 5 mL of water under rigorous stirring for a couple of hours. The reaction mixture was then taken up into $\sim$ 20 mL of dichloromethane and extracted three times with $NaHSO_4$ (20 mL) and three times with brine (20 mL). The organic layer was dried with $MgSO_4$, the solvent was evaporated, dissolved in a DMF (10 mL), filtered with a centriplus centrifugal filter (3000 MW cutoff),

precipitated into water, filtered, dried, dissolved in a small amount of CH_2Cl_2, precipitated into hexane, filtered, and dried to yield the product, **16**, as a white solid (0.10 g, 17%).

^{1}H NMR ($CDCl_3$) δ 0.8–2.0 (broad m, PMMA C**H**, CH_2, C**H$_3$**, octyl C**H$_2$**, PC**H$_2$**CH_2 and PCH_2C**H$_2$**), 2.63 (t, J = 7.2 Hz, C**H$_2$**COO) 3.1–3.8 (broad m, PMMA OC**H$_3$**), 3.9–4.1 (m, C**H$_2$**O, C**H$_2$**COO) ^{13}C NMR ($CDCl_3$): δ 13.93, 16.31, 18,62, 21.52, 22.45, 24.86, 28 89, 30.88, 31.15, 31.62, 44.36, 44.71, 51.64, 54.24, 176.77, 177.65, 177.93. ^{31}P NMR ($CDCl_3$): δ 48.70.

4-Azidobutanoic Anhydride, 18

To a stirred solution of 4-azidobutanoic acid (14.35 g, 111.1 mmol) in dichloromethane (50 mL), 1,3-dicyclohexylcarbodiimide (DCC) (11.46 g, 55.7 mmol) was added. The reaction mixture was stirred at room temperature over night, filtered, and evaporated to dryness. The byproducts were isolated through precipitation into ether (20 mL) and filtration. After evaporation, the product, **18**, was obtained as a colorless oil (12.9 g, 97%).

^{1}H NMR ($CDCl_3$): δ 1.94 (quin, J = 7.0 Hz, C**H$_2$**CH_2—N_3, 4H), 2.54 (t, J = 7.0 Hz, CH_2C**H$_2$**—N_3, 4H), 3.40 (t, J = 6.6 Hz, C**H$_2$**COO, 4H). ^{13}C NMR ($CDCl_3$): δ 23.54 (s, **C**H_2CH_2—N_3, 2C), 32.08 (s, CH_2**C**H_2—N_3, 2C), 50.15 (s, **C**H_2COO, 2C), 168.41 (s, CH_2**C**OO, 2C).

General Procedure for Functionalizing with Azides, Exemplified with $(N_3)_2$-G1-PMMA, 28

To a stirred solution of $(HO)_2$-G1-PMMA, **24** (2.03 g, 0.41 mmol), DMAP (20 mg, 0.16 mmol, 0.2 eq/OH), and pyridine (0.32 g, 4.1 mmol, 5 eq/OH) in 10 mL of CH_2Cl_2, 4-azidobutanoic anhydride, **18** (0.97 g, 4.10 mmol, 5 eq/OH) was added. The reaction was stirred overnight at RT. The residual anhydride was quenched by reaction with $\sim$ 10 mL of water under vigorous stirring for 2 h. The reaction mixture was then taken up into $\sim$ 150 mL of dichloromethane and extracted three times with $NaHSO_4$ (50 mL), three times with $NaHCO_3$ (50 mL), and finally once with brine (50 mL). The organic layer was dried with $MgSO_4$, the solvent was evaporated, and the crude product was dissolved in a small amount of CH_2Cl_2, precipitated into hexane, filtered, and dried to yield **28** as a pink solid (93%).

^{1}H NMR ($CDCl_3$) δ 0.8–2.1 (broad m, C**H$_2$**CH_2—N_3, PMMA C**H**, CH_2, C**H$_3$**), 2.4 (t, CH_2C**H$_2$**—N_3, J = 7.4 Hz), 3.4 (t, C**H$_2$**COO, J = 7.4 Hz), 3.1–3.8 (broad m, PMMA OC**H$_3$**), 3.9–4.1 (m, C**H$_2$**O, C**H$_2$**COO), 7.25–7.50 (m, *m,p-Ar***H**CSS and *o*,m,*p*-Ar), 8.0 (dd, J = 7.2 Hz, *o-Ar***H**CSS) ^{13}C NMR ($CDCl_3$): δ 14.22, 16.61, 18.82, 22.75, 31.96, 44.62, 44.97, 51.90, 54.56, 177.00, 177.91, 178.21.

$(N_3)_4$-G2-PMMA, 29

Following a similar procedure as for $(N_3)_2$-G1-PMMA, **28**, the second generation derivative, **29**, was obtained as a pink solid.

^{1}H NMR ($CDCl_3$) δ 0.8–2.1 (broad m, C**H$_2$**CH_2—N_3, PMMA C**H**, CH_2, C**H$_3$**), 2.4 (t, CH_2C**H$_2$**—N_3, J = 7.0 Hz), 3.4 (t, C**H$_2$**COO, J = 7.0 Hz), 3.1–3.8 (broad m, PMMA OC**H$_3$**), 3.9–4.1 (m, C**H$_2$**O, C**H$_2$**COO), 7.25–7.50 (m, *m,p-Ar***H**CSS and *o*,m,*p*-Ar), 8.0 (dd, J = 7.2 Hz, *o-Ar***H**CSS) ^{13}C NMR ($CDCl_3$): δ 14.20, 18.86, 22.75, 24.40, 31.68, 44.62, 44.96, 50.58, 51.91, 177.91, 178.21.

$(N_3)_8$-G3-PMMA, 30

Following a similar procedure as for $(N_3)_2$-G1-PMMA, **28**, the third generation derivative, **30**, was obtained as a pink solid.

^{1}H NMR ($CDCl_3$) δ 0.8–2.1 (broad m, C**H$_2$**CH_2—N_3, PMMA C**H**, CH_2, C**H$_3$**), 2.4 (t, CH_2C**H$_2$**—N_3, J = 7.5 Hz), 3.4 (t, C**H$_2$**COO, J = 7.5 Hz), 3.1–3.8 (broad m, PMMA OC**H$_3$**), 3.9–4.1 (m, C**H$_2$**O, C**H$_2$**COO), 7.25–7.50 (m, *m,p-Ar***H**CSS and *o*,m,*p*-Ar), 8.0 (dd, J = 7.0 Hz, *o-Ar***H**CSS) ^{13}C NMR ($CDCl_3$): δ 14.19, 16.37, 17.83, 18.81, 22.72, 24.18, 30.90, 31.65, 44.60,44.94, 50.56, 51.88, 54.47, 65.17, 172.18, 177.05, 177.88, 178.17.

General Procedure for Functionalizing with Phosphoric Acid Exemplified with $(H_2PO_4)_4$-G2-PMMA, 19

To a stirred solution of propargyl phosphoric acid (174 mg, 1.28 mmol, 2 eq/N_3), $(N_3)_4$-G2-PMMA, **29** (800 mg, 0.16 mmol), and diisopropylethylamine (DIPEA) (410 mg, 3.2 mmol, 5 eq/N_3) in 1.5 mL of DMF, $Cu(PPh_3)_3$ (15 mg, 0.016 mmol) was added. The crude polymer was precipitated into hexane, filtered, dissolved in 10 mL of CH_2Cl_2, extracted three times with 1 M HCl (5 mL), three times with $NaHCO_3$ (5 mL), and three times with 1 M HCl (5 mL). The organics were dried with $MgSO_4$, evaporated, dissolved in a small amount (milliliters) of CH_2Cl_2, precipitated into hexane, filtered, and dried to yield a pink solid, **19** (64%).

^{1}H NMR (DMSO) δ 0.8–2.1 (broad m, C**H$_2$**CH_2— PMMA C**H**, CH_2, C**H$_3$**), 2.4 (t,

$CH_2C\mathbf{H_2}$—, J = 6.9 Hz) , 3.4 (t, $C\mathbf{H_2}COO$, J = 6.9 Hz), 3.1–3.8 (broad m, PMMA $OC\mathbf{H_3}$), 3.9–4.1 (m, $C\mathbf{H_2}O$, $C\mathbf{H_2}COO$), 7.25–7.50 (m, *m,p-Ar***H**CSS and *o*,m,*p*-Ar), 8.0 (dd, J = 7.0 Hz, *o-Ar***H**CSS) ^{31}P NMR (DMSO): δ −1.01, −1.31.

$(H_2PO_4)_8$-G3-PMMA, 31

Following a similar procedure as for $(H_2PO_4)_4$-G2-PMMA, **19**, the third generation derivative, **31**, was obtained as a pink solid.

^{1}H NMR (DMSO) δ 0.8–2.1 (broad m, $C\mathbf{H_2}CH_2$—, PMMA C**H**, CH_2, $C\mathbf{H_3}$), 2.4 (t, $CH_2C\mathbf{H_2}$, J = 7.6 Hz), 3.4 (t, $C\mathbf{H_2}COO$, J = 7.6 Hz), 3.1–3.8 (broad m, PMMA $OC\mathbf{H_3}$), 3.9–4.1 (m, $C\mathbf{H_2}O$, $C\mathbf{H_2}COO$), 7.25–7.50 (m, *m,p-Ar***H**CSS and *o*,m,*p*-Ar), 8.0 (dd, J = 7.5 Hz, *o-Ar***H**CSS) ^{31}P NMR (DMSO): δ −0.99, −1.33.

Acetonide-G1-P(Bz-TEMA), 32

Following a similar procedure as for acetonide-G1-RAFT and using 2-(thiobenzyl)ethyl methacrylate as the monomer, the first generation derivative, **32**, was obtained as a pink solid.

^{1}H NMR ($CDCl_3$) δ 0.3–2.1 (broad m, P(Bz-TEMA)), 1.12 (s, $CC\mathbf{H_3}$), 1.34 (s, $CC\mathbf{H_3}$), 2.2–2.6 (broad s, P(Bz-TEMA)), 3.1–4.2 (broad m, $C\mathbf{H_2}O$, $C\mathbf{H_2}COO$ P(Bz-TEMA)), 6.7–7.50 (m, *m,p-Ar***H**CSS and *o*,m,*p*-Ar, P(Bz-TEMA)), 8.0 (dd, J = 7.4 Hz, *o-Ar***H**CSS). ^{13}C NMR ($CDCl_3$): δ 13.86, 17.02, 18.78, 19.38, 29.12, 29.25, 36.26, 36.33, 44.80, 45.16, 54.14, 63.80, 126.74, 127.26, 128.67, 128.97, 137.96, 176.38, 177.12, 177.96.

Acetonide-G2-P(Bz-TEMA), 8b

Following a similar procedure as for acetonide-G1-RAFT and using 2-(thiobenzyl)ethyl methacrylate as the monomer, the second generation derivative, **8b**, was obtained as a pink solid.

^{1}H NMR ($CDCl_3$) δ 0.3–2.1 (broad m, P(Bz-TEMA)), 1.12 (s, $CC\mathbf{H_3}$), 1.34 (s, $CC\mathbf{H_3}$), 2.2–2.6 (broad s, P(Bz-TEMA)), 3.1–4.2 (broad m, $C\mathbf{H_2}O$, $C\mathbf{H_2}COO$ P(Bz-TEMA)), 6.7–7.50 (m, *m,p-Ar***H**CSS and *o*,m,*p*-Ar, P(Bz-TEMA)), 8.0 (dd, J = 7.4 Hz, *o-Ar***H**CSS). ^{13}C NMR ($CDCl_3$): δ 16.92, 18.68, 19.37, 29.11, 29.11, 29.24, 36.25, 36.32, 44.80, 45.16, 63.78, 127.25, 128.66, 128.96, 137.95, 176.33, 177.10, 177.46.

Acetonide-G3-P(Bz-TEMA), 33

Following a similar procedure as for acetonide-G1-RAFT and using 2-(thiobenzyl)ethyl methacrylate as the monomer, the third generation derivative, **33**, was obtained as a pink solid.

^{1}H NMR ($CDCl_3$) δ 0.3–2.1 (broad m, P(Bz-TEMA)), 1.12 (s, $CC\mathbf{H_3}$), 1.34 (s, $CC\mathbf{H_3}$), 2.2–2.6 (broad s, P(Bz-TEMA)), 3.1–4.2 (broad m, $C\mathbf{H_2}O$, $C\mathbf{H_2}COO$ P(Bz-TEMA)), 6.7–7.50 (m, *m,p-Ar***H**CSS and *o*,m,*p*-Ar, P(Bz-TEMA)), 8.0 (dd, J = 7.4 Hz, *o-Ar***H**CSS). ^{13}C NMR ($CDCl_3$): δ 16.98, 18.53, 19.37, 29.11, 29.25, 36.25, 26.32, 42.05, 44.81, 45.16, 54.17, 63.80, 65.95, 98.12, 127.25, 128.66, 128.96, 137.96, 138.30, 176.38, 177.11, 177.45.

$(HO)_2$-G1-P(Bz-TEMA), 34

Following a similar deprotection procedure as for acetonide-G1-RAFT, the first generation derivative, **34**, was obtained as a pink solid.

^{1}H NMR ($CDCl_3$) δ 0.3–2.1 (broad m, P(Bz-TEMA)), 1, 2.2–2.6 (broad s, P(Bz-TEMA)), 3.1–4.2 (broad m, $C\mathbf{H_2}O$, $C\mathbf{H_2}COO$ P(Bz-TEMA)), 6.7–7.50 (m, *m,p-Ar***H**CSS and *o*,m,*p*-Ar, P(Bz-TEMA)), 8.0 (dd, J = 7.4 Hz, *o-Ar***H**CSS).

$(HO)_4$-G2-P(Bz-TEMA), 9b

Following a similar deprotection procedure as for acetonide-G1-RAFT, the second generation derivative, **9b**, was obtained as a pink solid.

^{1}H NMR ($CDCl_3$) δ 0.3–2.1 (broad m, P(Bz-TEMA)), 1, 2.2–2.6 (broad s, P(Bz-TEMA)), 3.1–4.2 (broad m, $C\mathbf{H_2}O$, $C\mathbf{H_2}COO$ P(Bz-TEMA)), 6.7–7.50 (m, *m,p-Ar***H**CSS and *o*,m,*p*-Ar, P(Bz-TEMA)), 8.0 (dd, J = 7.4 Hz, *o-Ar***H**CSS).

$(HO)_8$-G3-P(Bz-TEMA), 35

Following a similar deprotection procedure as for acetonide-G1-RAFT, the third generation derivative, **35**, was obtained as a pink solid.

^{1}H NMR ($CDCl_3$) δ 0.3–2.1 (broad m, P(Bz-TEMA)), 1, 2.2–2.6 (broad s, P(Bz-TEMA)), 3.1–4.2 (broad m, $C\mathbf{H_2}O$, $C\mathbf{H_2}COO$ P(Bz-TEMA)), 6.7–7.50 (m, *m,p-Ar***H**CSS and *o*,m,*p*-Ar, P(Bz-TEMA)), 8.0 (dd, J = 7.4 Hz, *o-Ar***H**CSS).

$(HOOC)_2$-G1-P(Bz-TEMA), 36

Following a similar acylation procedure as for $(HO)_2$-G1-RAFT, the first generation derivative, **36**, was obtained as a pink solid.

^{1}H NMR ($CDCl_3$) δ 0.3–2.1 (broad m, P(Bz-TEMA)), 1, 2.2–2.6 (broad s, P(Bz-TEMA), $C\mathbf{H_2}C\mathbf{H_2}COOH$), 3.1–4.2 (broad m, $C\mathbf{H_2}O$, $C\mathbf{H_2}COO$ P(Bz-TEMA)), 6.7–7.50 (m, *m,p-*

*Ar***H**CSS and *o*,m,*p*-Ar, P(Bz-TEMA)), 8.0 (dd, J = 7.4 Hz, *o*-*Ar***H**CSS). ^{13}C NMR ($CDCl_3$): δ 17.00, 18.78, 19.37, 29.10, 29.23, 30.35, 36.24, 36.31, 44.80, 45.15, 54.11, 63.81, 127.26, 128.96, 137.95, 176.37, 177.34, 177.47.

$(HOOC)_4$-G2-P(Bz-TEMA), 10b

Following a similar acylation procedure as for $(HO)_2$-G1-RAFT, the second generation derivative, **10b**, was obtained as a pink solid.

^{1}H NMR ($CDCl_3$) δ 0.3–2.1 (broad m, P(Bz-TEMA)), 1, 2.2–2.6 (broad s, P(Bz-TEMA), C**H$_2$**C**H$_2$**COOH), 3.1–4.2 (broad m, C**H$_2$**O, C**H$_2$**COO P(Bz-TEMA)), 6.7–7.50 (m, *m,p*-*Ar***H**CSS and *o*,m,*p*-Ar, P(Bz-TEMA)), 8.0 (dd, J = 7.4 Hz, *o*-*Ar***H**CSS). ^{13}C NMR ($CDCl_3$): δ 16.90, 18.68, 29.11, 29.24, 30.35, 36.32, 44.80, 45.12, 54.16, 63.79, 127.26, 128.67, 128.96, 138.00, 176.38, 177.32, 177.47.

$(HOOC)_8$-G3-P(Bz-TEMA), 37

Following a similar acylation procedure as for $(HO)_2$-G1-RAFT, the third generation derivative, **36**, was obtained as a pink solid.

^{1}H NMR ($CDCl_3$) δ 0.3–2.1 (broad m, P(Bz-TEMA)), 1, 2.2–2.6 (broad s, P(Bz-TEMA), C**H$_2$**C**H$_2$**COOH), 3.1–4.2 (broad m, C**H$_2$**O, C**H$_2$**COO P(Bz-TEMA)), 6.7–7.50 (m, *m,p*-*Ar***H**CSS and *o*,m,*p*-Ar, P(Bz-TEMA)), 8.0 (dd, J = 7.4 Hz, *o*-*Ar***H**CSS). ^{13}C NMR ($CDCl_3$): δ 16.93, 28.41, 29.15, 29.58, 30.33, 36.29, 44.78, 45.11, 51.83, 63.78, 124.20, 127.20, 128.65, 128.95, 137.95, 175.84, 177.12, 177.47.

Acetonide-G2-PS, 38

Following a similar procedure as for acetonide-G1-RAFT and using styrene as the monomer, the second generation derivative, **38**, was obtained as a pink solid.

^{1}H NMR δ 0.55 (t, $CH_2C\mathbf{H_3}$) 0.7–2.3 (broad m, PS C**H**, CH_2), 1.11 (s, CC**H$_3$**)1.32 (s, CC**H$_3$**), 3.5–4.3 (m, C**H$_2$**O, C**H$_2$**COO), 6–7.50 (m, *m,p*-*Ar***H**CSS and *o*,m,*p*-Ar, PS *ArH*), 8.0 (dd, J = 7.4 Hz, *o*-*Ar***H**CSS) ^{13}C NMR ($CDCl_3$): δ 18.48, 40.39, 44.22, 66.01, 68.02, 98.11, 125.68, 127.69, 128.00, 145.31.

$(HO)_4$-G2-PS, 39

Following a similar deprotection procedure as for acetonide-G1-RAFT, the second generation polystyrene derivative, **39**, was obtained as a pink solid.

^{1}H NMR δ 0.55 (t, $CH_2C\mathbf{H_3}$) 0.7–2.3 (broad m, PS C**H**, CH_2), 3.5–4.3 (m, C**H$_2$**O, C**H$_2$**COO), 6–7.50 (m, *m,p*-*Ar***H**CSS and *o*,m,*p*-Ar, PS *ArH*), 8.0 (dd, J = 7.4 Hz, *o*-*Ar***H**CSS) ^{13}C NMR ($CDCl_3$): δ 25.64, 30.35, 40.43, 68.01, 125.66, 127.68, 127.99, 145.22.

$(HOOC)_4$-G2-PS, 40

Following a similar acylation procedure as for $(HO)_2$-G1-RAFT, the second generation polystyrene derivative, **40**, was obtained as a pink solid.

^{1}H NMR δ 0.55 (t, $CH_2C\mathbf{H_3}$) 0.7–2.3 (broad m, PS C**H**, CH_2), 2.3–2.5 (broad s, C**H$_2$**C**H$_2$**COOH), 3.5–4.3 (m, C**H$_2$**O, C**H$_2$**COO), 6–7.50 (m, *m,p*-*Ar***H**CSS and *o*,m,*p*-Ar, PS *ArH*), 8.0 (dd, J = 7.4 Hz, *o*-*Ar***H**CSS) ^{13}C NMR ($CDCl_3$): δ 40.47, 44.23, 45.94, 125.59, 126.28, 127.73, 128.05, 145.18, 145.71.

The authors gratefully acknowledge the financial support from the Mitsubishi Chemical Center for Advanced Materials and the UCSB Materials Research Laboratory (NSF Grant DMR05-20415).

REFERENCES AND NOTES

1. (a) Vaia, R. A.; Maguire, J. F. Chem Mater 2007, 19, 2736–2751; (b) Shah, D.; Maiti, P.; Gunn, E.; Schmidt, D. F.; Jiang, D. D.; Batt, C. A.; Giannelis, E. P. Adv Mater 2004, 16, 1173–1177; (c) Tuteja, A.; Mackay, M. E.; Hawker, C. J.; Van Horn, B. Macromolecules 2005, 38, 8000–8011.
2. (a) Li, Y.-Q.; Fu, S.-Y.; Yang, Y.; Mai, Y.-W. Chem Mater 2008, 20, 2637–2643; (b) Liu, J.; Nakamura, Y.; Ogura, T.; Shibasaki, Y.; Ando, S.; Ueda, M. Chem Mater 2008, 20, 273–281; (c) Boettcher, S. W.; Bartl, M. H.; Hu, J. G.; Stucky, G. D. J Am Chem Soc 2005, 127, 9721–9730; (d) Lu, C.; Guan, C.; Liu, Y.; Cheng, Y.; Yang, B. Chem Mater 2005, 17, 2448–2454.
3. (a) Hooper, J. B.; Schweizer, K. S. Macromolecules 2005, 38, 8858–8869; (b) Zhou, S.; Garnweitner, G.; Niederberger, M.; Antonietti, M. Langmuir 2007, 23, 9178–9187; (c) Corbierre, M. K.; Cameron, N. S.; Sutton, M.; Laaziri, K.; Lennox, R. B. Langmuir 2005, 21, 6063–6072.
4. (a) Zhang, Q.; Russell, T. P.; Emrick, T. Chem Mater 2007, 19, 3712–3716; (b) Costanzo, P. J.; Demaree, J. D.; Beyer, F. L. Langmuir 2006, 22, 10251–10257; (c) Ha, Y.-H.; Kwon, Y.; Breiner, T.; Chan, E. P.; Tzianetopoulou, T.; Cohen, R. E.; Boyce, M. C.; Thomas, E. L. Macromolecules 2005, 38, 5170–5179; (d) Selvan, S. T.; Hayakawa, T.; Nogami, M.; Moller, M. J Phys Chem B 1999, 103, 7441–7448.

5. Leduc, M. R.; Hawker, C. J.; Dao, J.; Fréchet, J. M. J. J Am Chem Soc 1996, 118, 11111–11118.
6. Gitsov, I. J Polym Sci Part A: Polym Chem 2008, 46, 5295–5314.
7. Iyer, J.; Fleming, K.; Hammond, P. T. Macromolecules 1998, 31, 8757–8765.
8. (a) Mecerreyes, D.; Dubois, P.; Jérôme, R.; Hedrick, J. L.; Hawker, C. J. J Polym Sci Part A: Polym Chem 1999, 37, 1923–1930; (b) Matyjaszewski, K.; Shigemoto, T.; Fréchet, J. M. J.; Leduc, M. Macromolecules 1996, 29, 4167–4171.
9. (a) Knecht, M. R.; Weir, M. G.; Myers, V. S.; Pyrz, W. D.; Ye, H.; Petkov, V.; Buttrey, D. J.; Frenkel, A. I.; Crooks, R. M. Chem Mater 2008, 20, 5218–5228; (b) Huang, W.; Kuhn, J. N.; Tsung, C.-K.; Zhang, Y.; Habas, S. E.; Yang, P.; Somorjai, G. A. Nano Lett 2008, 8, 2027–2034; (c) Shi, X.; Sun, K.; Baker, J. R., Jr. J Phys Chem C 2008, 112, 8251–8258.
10. van Hest, J. C. M.; Baars, M. W. P. L.; Elissen-Román, C.; van Genderen, M. H. P.; Meijer, E. W. Macromolecules 1995, 28, 6689–6691.
11. Groehn, F.; Gu, X.; Gruell, H.; Meredith, J. C.; Nisato, G.; Bauer, B. J.; Karim, A.; Amis, E. J. Macromolecules 2002, 35, 4852–4854.
12. Pathak, S.; Singh Anup, K.; McElhanon James, R.; Dentinger Paul, M. Langmuir 2004, 20, 6075–6079.
13. McCain, K. S.; Schluesche, P.; Harris, J. M. Anal Chem 2004, 76, 930–938.
14. (a) Liebau, M.; Janssen, H. M.; Inoue, K.; Shinkai, S.; Huskens, J.; Sijbesma, R. P.; Meijer, E. W.; Reinhoudt, D. N. Langmuir 2002, 18, 674–682; (b) Pochan, D. J.; Pakstis, L.; Huang, E.; Hawker, C.; Vestberg, R.; Pople, J. Macromolecules 2002, 35, 9239–9242; (c) Connal, L. A.; Vestberg, R.; Gurr, P. A.; Hawker, C. J.; Qiao, G. G. Langmuir 2008, 24, 556–562; (d) Pyun, J.; Tang, C.; Kowalewski, T.; Frechet, J. M. J.; Hawker, C. J. Macromolecules 2005, 38, 2674–2685; (e) Kampf, J. P.; Frank, C. W.; Malmstrom, E. E.; Hawker, C. J. Langmuir 1999, 15, 227–233.
15. Fréchet, J. M. J.; Gitsov, I.; Monteil, T.; Rochat, S.; Sassi, J.-F.; Vergelati, C.; Yu, D. Chem Mater 1999, 11, 1267–1274.
16. (a) Lohse, B.; Vestberg, R.; Ivanov, M. T.; Hvilsted, S.; Berg, R. H.; Ramanujam, P. S.; Hawker, C. J. J Polym Sci Part A: Polym Chem 2007, 45, 4401–4412; (b) Vestberg, R.; Malkoch, M.; Kade, M.; Wu, P.; Fokin, V. V.; Sharpless, K. B.; Drockenmuller, E.; Hawker, C. J. J Polym Sci Part A: Polym Chem 2007, 45, 2835–2846.
17. (a) Nyström, A. M.; Malmström, E.; Hult, A. J Polym Sci Part A: Polym Chem 2005, 43, 4496–44504; (b) Malkoch, M.; Malmström, E.; Hult, A. Macromolecules 2002, 35, 8307–8314; (c) Ihre, H.; Hult, A.; Fréchet, J. M. J.; Gitsov, I. Macromolecules 1998, 31, 4061–4068; (d) Nilsson, C.; Simpson, N.; Malkoch, M.; Johansson, M.; Malmström, E. J Polym Sci Part A: Polym Chem 2008, 46, 1339–1348.
18. (a) Barner-Kowollik, C.; Perrier, S. J Polym Sci Part A: Polym Chem 2008, 46, 5715–5723; (b) Nguyen, T. L. U.; Farrugia, B.; Davis, T. P.; Barner-Kowollik, C.; Stenzel, M. H. J Polym Sci Part A: Polym Chem 2007, 45, 3256–3272; (c) Gemici, H.; Legge, T. M.; Whittaker, M.; Monteiro, M. J.; Perrier, S. J Polym Sci Part A: Polym Chem 2007, 45, 2334–2340.
19. (a) Williams, S. R.; Mather, B. D.; Miller, K. M.; Long, T. E. J Polym Sci Part A: Polym Chem 2007, 45, 4118–4128; (b) Venkataraman, S.; Wooley, K. L. J Polym Sci Part A: Polym Chem 2007, 45, 5420–5430; (c) Skey, J.; O'Reilly, R. K. J Polym Sci Part A: Polym Chem 2008, 46, 3690–3702.
20. Kim, B. J.; Given-Beck, S.; Bang, J.; Hawker, C. J.; Kramer, E. J. Macromolecules 2007, 40, 1796–1798.
21. Williams, R. H.; Hamilton, L. A. J Am Chem Soc 1952, 74, 5418–5420.
22. Antoni, P.; Nystrom, D.; Hawker, C. J.; Hult, A.; Malkoch, M. Chem Commun 2007, 2249–2251.
23. Rostovtsev, V. V.; Green, L. G.; Fokin, V. V.; Sharpless, K. B. Angew Chem Int Ed Engl 2002, 41, 2596–2599.
24. Malkoch, M.; Schleicher, K.; Drockenmuller, E.; Hawker, C. J.; Russell, T. P.; Wu, P.; Fokin, V. V. Macromolecules 2005, 38, 3663–3678.
25. Skaff, H.; Emrick, T. Angew Chem Int Ed Engl 2004, 43, 5383–5386.
26. Turkevich, J.; Stevenson, P. C.; Hillier, J. Discuss Faraday Soc 1951, 11, 55–75.
27. Merican, Z.; Schiller, T. L.; Hawker, C. J.; Fredericks, P. M.; Blakey, I. Langmuir 2007, 23, 10539–10545.
28. Gujadhur, R.; Venkataraman, D.; Kintigh, J. T. Tetrahedron Lett 2001, 42, 4791–4793.
29. Moore, J. S.; Stupp, S. I. Macromolecules 1990, 23, 65–70.
30. Khoukhi, N.; Vaultier, M.; Carrie, R. Tetrahedron 1987, 43, 1811–1822.